Addis Ababa University

College of Health Sciences School of Pharmacy

Department of Pharmaceutical Chemistry and Pharmacognosy

Synthesis, Antimicrobial, and *In silico* Studies of 2-Hydroxy-1, 2-Diphenylethanone Derivatives

By: Temesgen Kusse (B. Pharm)

Advisors: Dr. Daniel Bisrat (PhD)

Prof. Kaleab Asres (PhD)

June, 2025

Addis Ababa, Ethiopia

College of Health Sciences

School of Pharmacy

Department of Pharmaceutical Chemistry and Pharmacognosy

Synthesis, Antimicrobial, and *In silico* Studies of 2-Hydroxy-1, 2-Diphenylethanone Derivatives

By: Temesgen Kusse (B. Pharm)

A Thesis Submitted to the Department of Pharmaceutical Chemistry and Pharmacognosy, in Partial fulfillment of the Requirements for the Degree of Master of Science in Medicinal Chemistry.

Advisors: Dr. Daniel Bisrat (PhD.)

Prof. Kaleab Asres (PhD.)

June 2025

Addis Ababa, Ethiopia

Addis Ababa University

School of Graduate Studies

This is to certify that the thesis prepared by Temesgen Kusse (B. Pharm) entitled "**Synthesis, Antimicrobial, and *In silico* Studies of 2-Hydroxy-1, 2-diphenylethanone Derivatives"** and submitted in partial completion of the criteria for the Degree Master of Science in Medicinal Chemistry conforms with university norms and satisfies recognized standards for quality and originality.

Signed by the Examining Committee:

External examiner: Dr. Wondimageng Tamiru (PhD) Signature _____Date_____

Internal examiner: Mr. Alemu Tadesse (MSc.) Signature _____Date_____

Advisors:

Dr. Daniel Bisrat (PhD.) Signature _____Date_____

Prof. Kaleab Asres (PhD.) Signature _____Date_____

_____

Chair of the Department

ACKNOWLEDGMENT

First of all, I would like to take this opportunity to express my great thanks to our all-thing, Jesus Christ; who was, who is and who will be with me yesterday, today and tomorrow. I will do not have a single word or phrase or sentence which is equivalent to His help, but Let His name will be blessed forever.

Next, I extend my heartfelt gratitude to Department of Pharmaceutical chemistry and Pharmacognosy, School of Pharmacy, College of Health Sciences Addis Ababa University for funding my research, deep regard goes to our advisor to Dr Daniel Bisrat (PhD) & Prof. Kaleab Asres (PhD) for their exemplary guidance, and valuable feedback throughout the duration of my paper. There valuable suggestions will of great help throughout our paper work.

I am especially grateful to Prof. Avijit Mazumder for conducting the antimicrobial experiments. My deepest gratitude is extended to my family, friends, and everyone else who helped me finish this research project successfully.

ABBREVIATION AND ACRONYM

^{13}C-NMR	^{13}C-Nuclear Magnetic Resonance
^{1}H-NMR	Proton Nuclear Magnetic Resonance
ADMET	Absorption, Distribution, Metabolism, Excretion and Toxicity
AMR	Anti-Microbial Resistance
BBB	Blood Brain Barrier
BPPL	Bacterial Priority Pathogens List
Caco-2	Human Colon Adenocarcinoma Cell Lines,
$CDCl_3$	Detureted chloroform
CL	Clearance
CYP450	Cytochromes P450
DMSO	Dimethyl Sulfoxide
DsbA	Disulfide bond
Fsp^3	number of sp3 hybridized carbons,
hERG	Human Ether-A-Go-Go Related Gene
H-HT	Human Hepatotoxicity
HIA	Human Intestinal Absorption;
LR-5	Lipinski rule of 5,
MDR	Multi-Drug Resistance
MIC	Minim Inhibitatory Concentration
nHA	number of hydrogen bond acceptors
nHD	number of hydrogen bond donors
nRot	number of rotatable bonds,
^{O}C	Degree celicous
PAINS	Pan Assay Interference Compounds
PDB	Protein Data Bank
P-gp	P-glycoprotein
Pgp-inhib	P-glycoprotein inhibitor,
PPB	Plasma Protein Binding
QED	Measure of Drug-Likeness,
Rpm	revolutions per minute
SA score	Synthetic Accessibility Score,

SMILES	Simplified Molecular Input Line Entry System
$t_{½}$	half-life;
TDOR	Thiol Disulfide Oxidoreductase
TLC	Thin Layer Chromatography
TPSA	Topological Polar Surface Area,
USA	United State of America
UV	Ultra Violet
VD	Volume of distribution;
WHO	World Health Organization

TABLE OF CONTENT

LIST OF FIGURES

LIST OF SCHEMES

LIST OF TABLES

ABSTRACT

Synthesis, Antimicrobial, and *In silico* Studies of 2-Hydroxy-1, 2-Diphenylethanone Derivatives

Infectious diseases place a significant impact on the healthcare system. It causes 7.7 million fatalities each year, with a disproportionately high burden in sub-Saharan Africa. Drug resistant pathogens attributed to 4.95 million are and 1.27 million are brought on by illnesses of bacteria that are resistant to the current medications. Therefore, there is an urgent need for new, safe, and effective compounds to combat antimicrobial resistance (AMR). In this context, 2-hydroxy-1,2-diphenylethanone has emerged as a valuable precursor in medicinal chemistry, attracting significant interest for the development of novel bioactive molecules. The aim of this study was to synthesize new compounds derived from 2-hydroxy-1,2-diphenylethanone using the Mannich reaction and to evaluate their antibacterial and antifungal activities against 26 bacterial strains and 4 fungal strains. Three compounds were successfully synthesized and their structures were confirmed as 2-hydroxy-1,2-diphenyl-3-(piperidin-1-yl)propan-1-one (**20**), 1-(2-hydroxy-3-oxo-2,3-diphenylpropyl)urea **(21),** and 3-(diethylamino)-2-hydroxy-1,2-diphenylpropan-1-one **(22)** using ^{1}H and ^{13}C-NMR spectroscopy. All the synthesized compounds exhibited broad-spectrum antibacterial activity. Among them, compound **21** demonstrated the highest activity, with a minimum inhibitory concentration (MIC) of 10 μg/mL against *Shigella sonnei* 1, *Shigella boydii* D13629, and *Pseudomonas aeruginosa* MDR1. Furthermore, synthesized compounds exhibited Antifungal activity.

Among them, compound **21** demonstrated the highest activity, with a minimum inhibitory concentration (MIC) of 200 µg/mL against *Candida albicans* ATCC 10231, *Aspergillus niger* ATCC 6275, *Penicillium funiculosum* NCTC 287, and *Penicillium notatum* ATCC 11625. Molecular docking studies were performed to predict the potential mechanism of action of the synthesized compounds. The results showed that the compounds interact favorably with conserved residues in the binding site of *E. coli* DsbA (PDB ID: 8DN0) through hydrogen bonding and hydrophobic interactions, with docking scores of –7.5 kcal/mol (**21**), –7.1 kcal/mol (**22**), and –6.5 kcal/mol (**20**). The current study suggests that the three 2-hydroxy-1,2-diphenylethanone derivatives have potential as lead compounds for further optimization in the development of antimicrobial agents. However, additional studies are needed to assess their safety profiles through comprehensive toxicity testing.

Keywords: 2-Hydroxy-1, 2-diphenylethanone, Antimicrobial activity, *In-silico* studies, Disulfide bond oxidoreductase (DsbA), Mannich reaction

1. INTRODUCTION

1.1. Infectious Diseases

Infectious ailments are illnesses caused by dangerous microbes such as bacteria, viruses, fungi, or parasites that attack the body. They can spread in a variety of methods, including direct transmission from person to person, contact with contaminated objects, insect bites, and environmental exposure (Berkelman et al., 1994).

Globally, infectious diseases place a significant strain on the healthcare system. In 2022, infectious diseases affected around 900 million individuals, which resulted in an immense burden on the global healthcare system. It causes 7.7 million fatalities each year, of which 4.95 million are attributed to drug-resistant pathogens and 1.27 million are brought on by illnesses of bacteria that are resistant to the current medications (Okeke et al., 2024; Rathore et al., 2025). The main organisms causing infections globally include bacteria, fungi, viruses, and parasites (Hsueh et al., 2024).

With a disproportionately high burden in sub-Saharan Africa, infectious illnesses continue to pose a serious threat to public health. This is frequently brought on by elements including inadequate health systems, restricted access to care and the effects of socioeconomic inequality. It can be challenging to administer treatments to afflicted populations (Paul, 2024).

In Ethiopia, analysis revealed significant variations in antibiotic resistance across regions In Amhara, high resistance rates were observed for trimethoprim-sulfamethoxazole (82.88%) and meropenem (44.96%). In Addis Ababa, resistance was notably higher for

ciprofloxacin (64.78%) and cefotaxime (93.49%). In Oromia, higher resistance rates were observed for ceftazidime and trimethoprim-sulfamethoxazole, with 99.50% for each. Lastly, SNNPR exhibited lower resistance levels for trimethoprim-sulfamethoxazole at 34.07% and meropenem at 20.54%. This is resistance result need rational uses and search for new medication (Asmare et al., 2025).

1.1.1. Bacterial Infection

Single-celled microbes known as bacteria are found in most vertebrates, and many of them are beneficial. However, they can cause an infection that faces great problems in modern medicine, which range from asymptomatic to potentially fatal, and are brought on by common germs like bacteria (Pieniążek et al., 2024).

Human health is seriously threatened by bacterial infections. Because of the high morbidity and mortality rates associated with these infections, it is crucial to identify and treat harmful microorganisms promptly and efficiently (Deusenbery et al., 2021). Gram-negative bacteria were present, including *Acinetobacter baumannii Klebsiella pneumonia*, *Pseudomonas*, *Proteus*, *Salmonella Providencia Escherichia*, *Morganella* and *Pseudomonas aeruginosa* (Santoso et al., 2022).

1.1.2. Fungal Infection

Fungal infections remain a major public health concern because of their underestimated frequency and lack of recognition which often leads to delayed diagnoses and treatments. As a result, many individuals suffer from prolonged illness and complications that could have been prevented with timely intervention (Gnat et al., 2021).

Even though they are especially important to humans, they infiltrate human tissues and result in superficial, subcutaneous, or systemic illnesses to cause fungal diseases. Millions of people around the world are at serious risk from fungal infections like that of bacteria; fungal infections have become much more common in recent decades (Thambugala et al., 2024).

Currently, approximately 300 fungal species are known to cause human diseases, mostly in immune-compromised and immune-competent populations, especially those with chronic respiratory disorders and underlying co-morbidities, as well as those living in poverty (Bongomin et al., 2017).

The most common fungal infections are pulmonary *Aspergillosis*, *Candidiasis* bloodstream infection or invasive *candidiasis*, *Pneumocystis pneumonia*, *Cryptococcal* and other major life-threatening fungal infections. These an annual incidence of 6·5 million invasive fungal infections and 3·8 million deaths, of which about 2·5 million were directly attributable the fungi like *Aspergillosis*, *Candidiasis*, *Pneumocystosis*, and *Cryptococcal* meningitis (Denning, 2024; Mardani, 2024) are the come pathogens.

1.2. Drug Resistance

Drug resistance is a condition in which the viability or reproductive ability of microorganism is not affected after they are exposed to anti-microbial drugs that can affect the viability or reproductive ability of the microorganism (Chen, 2024). A growing threat to global health, antimicrobial resistance (AMR) is being measured increasing in terms of its impact on human health and the economy (Keenan et al., 2025).

There are 24 pathogens in the 2024 World Health Organization (WHO) Bacterial Priority Pathogens List (BPPL), representing 15 families of bacterial pathogens that are resistant to antibiotics. These include drug-resistant *mycobacterium* tuberculosis, Gram-negative bacteria resistant to last-resort antibiotics such as *Shigella*, *Salmonella*, *Neisseria gonorrhoeae*, *Pseudomonas aeruginosa*, and *Staphylococcus aureus*. In addition to issues with drug interactions and antimicrobial resistance, there is a lack of recently approved antibiotics on the market. The Research & Development pipeline for novel medicines and new resistance patterns are also reflected (WHO, 2024).

Bacterial AMR was expected to be responsible for 4·71 million fatalities in 2021, including 1·14 million deaths. Over the previous 31 years, trends in AMR mortality differed significantly by region and age. Between 1990 and 2021, the number of fatalities from AMR rose by more than 80% for people aged 70 and above, whereas it fell by more than 50% for children under the age of five (Naghavi et al., 2024).

1.3. Statement of the Problem

Antibiotics are among the most important medical advancements of the 20th century, having prevented illnesses that killed millions of people. Increased illness, death, and economic burden are the results of the emergence of AMR, which is a major danger to global public health (Naghavi et al., 2024).

A further factor in the issue is the lack of new antibiotics. The use of antibiotics in surveillance must be improved, access to high-quality medications and vaccinations strengthened, and regulations must be enforced to battle AMR. A possible post-antibiotic age must be avoided by a concerted, international effort (Salam et al., 2023).

The rapid emergence and global spread of AMR have rendered many existing antibiotics and antifungal agents ineffective, creating a significant public health threat. Infections caused by multi-drug resistance (MDR) bacteria and fungi are becoming increasingly difficult to treat, resulting in longer illness durations, higher medical costs, and increased mortality (Rather et al., 2021).

WHO BPPL, drug resistant *mycobacterium* tuberculosis, Gram-negative bacteria resistant to last-resort antibiotics such as *Shigella*, *Salmonella*, *Neisseria gonorrhoeae*, *Pseudomonas aeruginosa*, and *Staphylococcus aureus*, need for new antibiotics with new targets or new mechanisms of action is particularly, important in this microbial infection. In addition to antimicrobial resistance, there is a lack of recently approved antibiotics on the market from Research & Development pipeline for novel medicines and new resistance patterns are also reflected (WHO, 2024).

1.4.Significance of the Study

WHO, has highlighted an urgent need for the development of new antibiotics due to the rising threat of AMR and the declining availability of novel drugs (WHO, 2024).This need is especially critical in addressing infections caused by MDR pathogens commonly referred to as "superbugs" which continue to challenge current treatment options (Süssmuth et al., 2025)..

In response to this concern, the present study demonstrates the potential of synthesizing novel compounds derived from 2-hydroxy-1,2-diphenylethanone using the Mannich reaction. The synthesis method is not only cost-effective but also yields relatively high product quantities, making it accessible and scalable.

Secondly, synthesize new compounds that exhibite broad-spectrum antibacterial activity particularly, against MDR strains such as *Pseudomonas aeruginosa* MDR1, and also effective against WHO BPPL that are clinical important strains. Thirdly, unlike many existing antibiotics, which are limited by narrow-spectrum activity, these compounds were active against a wide range of bacterial strains, including polymicrobial infections. This broad activity enhances their potential as versatile candidates in the fight against complex infectious diseases.

Finally, the findings of this study provide a valuable foundation for future research in medicinal chemistry, offering both synthetic strategies and biological insights for the development of new antimicrobial agents.

2. OBJECTIVE OF THE STUDY

2.1. General objective

To synthesize derivatives of 2-hydroxy-1,2-diphenylethanone and evaluate their antimicrobial potential through *in vitro* assays and *in silico* molecular modeling studies.

2.2. Specific objectives

- To synthesize 2-hydroxy-1, 2-diphenylethanone derivatives via Mannich reaction
- To confirm the structural of the synthesized compounds using ^{1}H and ^{13}C-NMR spectroscopy.
- To evaluate *in vitro* antimicrobial activities of the synthesized compounds against 26 bacterial and 4 fungal strains using the disk diffusion and the broth dilution methods
- To perform *in silico* studies of 2-hydroxy-1, 2-diphenylethanone Derivatives.

3. LITERATURE REVIEW

3.1. Antimicrobial Activity of 2-Hydroxy-1, 2-Diphenylethanone Derivatives,

Benzoin (2-hydroxy-1,2-diphenylethanone) (**1**)and benzil (**2**)are important organic molecules that contain ketone, alcohol, and aromatic phenyl functional groups. These compounds display a wide range of pharmacological activities, including antimalarial, antifungal, antioxidant, anticancer, and antibacterial properties (Sarsamkar & Gramopadhye, 2021; Yaylı et al., 2022)

Benzoin is a natural product produced as a resin by *Styrax* trees and is commonly used as a flavoring agent, incense, and in perfumes. For thousands of years, it has been cultivated in many parts of the world for its traditional use in treating wounds, skin conditions, neurological disorders, anxiety, and muscle soreness (Atia Sharif et al., 2016; Fernández, 2004). People are becoming more interested in benzoin's and their derivatives because of their significance in the chemical industry and medicinal chemistry as a bridge for the synthesis of several essential organic functional groups and high-profile biologically active natural compounds (Babu Kothapalli et al., 2025).

So far, benzoin derivatives have also shown growth inhibition at extremely low concentrations in a variety of cancer cell lines, making them interesting options. Notably anti-tumor action against variety of malignancies including; breast, melanoma, colon, central nervous system tumors, prostate, lung, and other malignancies without causing cytotoxicity (Zaware et al., 2025).

Different compounds containing benzoin were synthesized by Schiff base-metal complexes, particularly copper and zinc. They can also conjugate with other structures

like sulfamethazine derivatives (**3**), hold considerable promise for developing new antimicrobial agents and as simple derivatives like benzoyl and benzil that have anti-microbial activity (Buran, 2025).

Previous studies have shown that the commonly used antifungal agent Nystatin, the antibacterial agent Kanamycin, and the synthetic compound N-(2-hydroxybenzylidene)-2'-hydroxyimine (**4**) exhibit strong antimicrobial activity (Jesmin et al., 2008). Several aerobic, anaerobic, and spore-forming bacteria, together with *Candida albicans* and *Mycobacterium fortuitism*, were treated by benzoin tincture solution. The only index organism that showed a distinct capacity to endure 15-minute incubation in benzoin tincture was *Bacillus cereus* (Okeke et al., 2024). Among the methoxy benzoin derivatives, benzil derivative was the most effective against *E. coli*, *Y. pseudotuberculosis*, *M. smegmatis*, and *C. albicans*, while the stilbenoid compound showed specific activity against *B. cereus* (Yaylı et al., 2021).

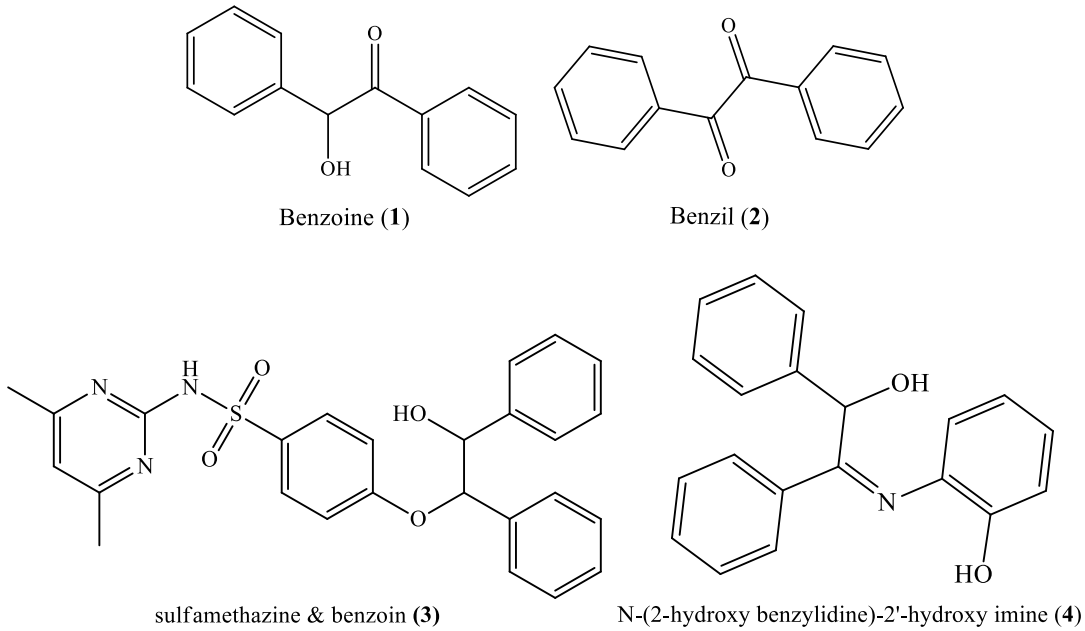

Figure 1: Different compounds contains benzoin

The other synthesized derivatives of benzoin involve substitutions on the aromatic rings of 2-hydroxy-1,2-diphenylethanone, resulting in the formation of methoxy benzoin derivatives (compounds **5–9**) and benzil derivatives (compounds **10–17**), as shown in Table 1 below. All benzil derivatives displayed bioactivity against *M. smegmatis* and *C. albicans.*

Table 1: Methoxy benzoin and benzil derivatives

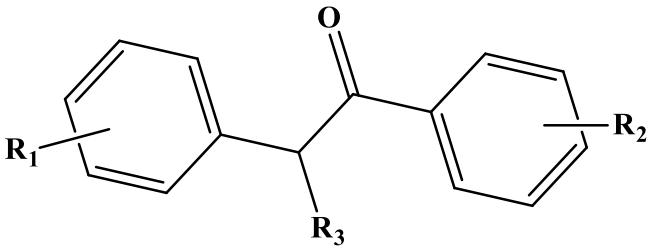

No	R_1	R_2	R_3
Hydroxy methoxy benzoin			
5	4 –OCH_3	3 –OH	OH
6	3, 4 –diOCH_3	3 –OH	OH
7	3 –OCH_3	4 –OH	OH
8	3, 5–diOCH_3	4 –OH	OH
9	3, 4–diOCH_3	3 –OH	OH
Hydroxy methoxy benzil			
10	3 –OCH_3	3 –OH	=O
11	4–OCH_3	3 –OH	=O
12	3, 4–diOCH_3	3 –OH	=O
13	3, 5–diOCH_3	3 –OH	=O
14	3 –OCH_3	4 –OH	=O
15	4–OCH_3	4 –OH	=O
16	3, 4–diOCH_3	4 –OH	=O
17	3, 5–diOCH_3	4 –OH	=O

3.2. Synthesis of 2-Hydroxy-1, 2-diphenylethanone Derivatives,

2-Hydroxy-1, 2-diphenylethanone derivatives, commonly known as benzoin, can be achieved through various methods. One notable approach involves benzoin condensation reactions typically involves the condensation of benzoin with amines to form Schiff base ligands (Saviour Iorungwa et al., 2019) and via the Mannich reaction.

In the Mannich reaction have three-component, a ketone, formaldehyde, and an amine react to create *β*-amino ketones. The amine functions as a nucleophile, attacking the formaldehyde's which is electrophilic carbon before being added to the ketone before generating final product (Blicke, 1942).

3.3. Potential target for 2-Hydroxy-1, 2-diphenylethanone Derivatives

Knowledge of targets within cellular and disease networks necessitates a systematic interrogation of the combination of drugs and their respective targets (Tolani et al., 2021). Targets may encompass enzymes, receptors, ion channels, or nucleic acids. (Eckels et al., 2021).

The cellular machinery seen in all organisms adds disulfide bonds to freshly generated proteins while they are being transported out of the cytoplasm to have folded structure of protein (Nassar et al., 2021). DsbA (Disulfide bond) is bacterial thiol disulfide oxidoreductase (TDOR) enzyme family that catalyzes intrachain disulfide bond formation.

This DsbA family present in different bacteria's like; *Klebsiella pneumonia*, *Vibrio cholera*, *Pseudomonas aeruginosa*, *Staphylococcus aureus*, *Neisseria meningitides*,

Bacillus subtili, *Wolbachia pipientis* and *Burkholderia pseudomallei* (Santos-Martin et al., 2021).

In *E. coli*, the membrane-integrated DsbB protein forms a disulfide bond with ubiquinone and transfers it to DsbA, a periplasmic dithiol oxidoreductase that acts as the direct giver of disulfide bonds to proteins folding oxidative in this compartment (Inaba & Ito, 2008) (see figure 2: below).

From a biochemical perspective, the role of DsbA is bacterial protein maturation, but it also has important ramifications for antimicrobial research. By blocking DsbA, important proteins' ability to make disulfide bonds correctly may be compromised like Attenuating bacterial virulence and undermining the Maturation of Proteins (Shouldice et al., 2011).

Different small-molecule inhibitors (compounds **18** and **19**) have been identified that selectively target DsbA enzymes in *E. coli*, with minimal activity against the human counterpart. These compounds alter cysteine and lysine residues on DsbA and DsbB in a manner that suggests a degree of selectivity, likely due to structural differences in the non-redox active sites (Halili et al., 2015).

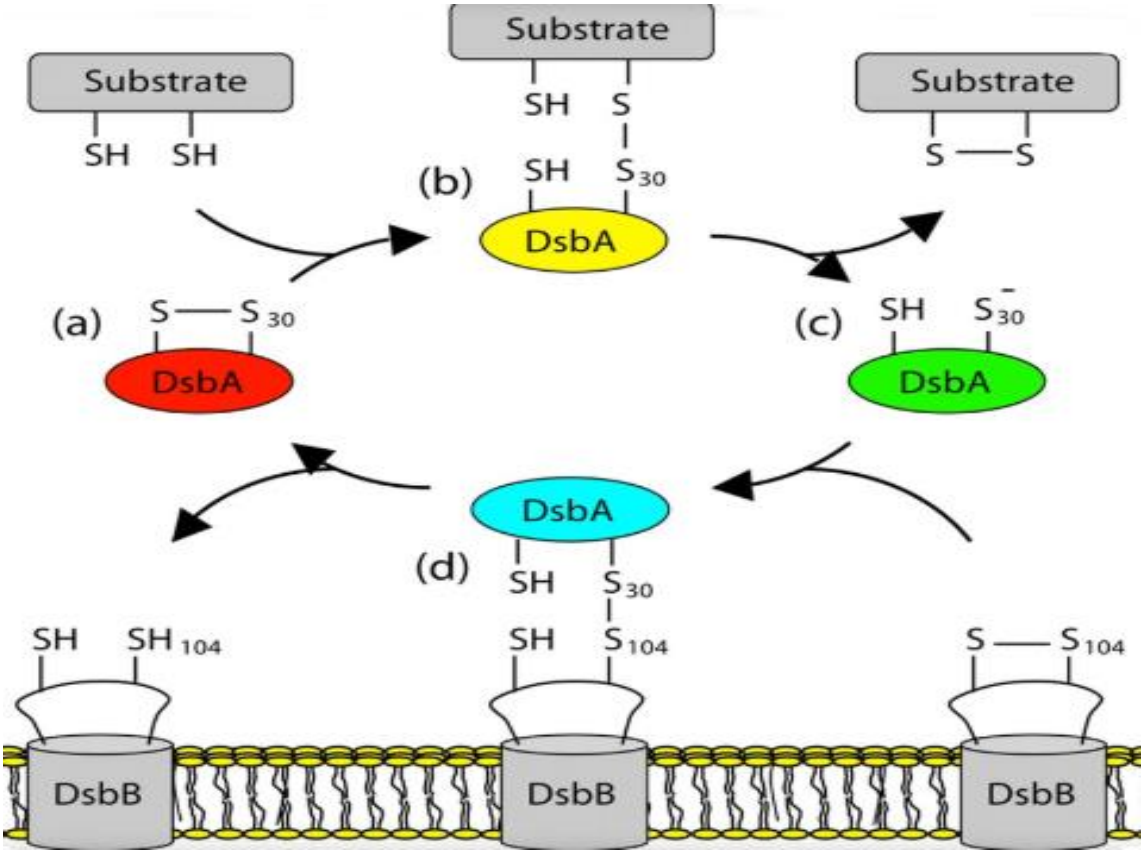

Figure 2: The catalytic cycle of DsbA

Key: ***(a),*** *oxidized DsbA reacts with a variety of substrate proteins to generate a mixed disulfide DsbA-substrate complex* ***(b),*** *The complex is rapidly resolved with release of oxidized substrate and reduced DsbA* ***(c),*** *Reduced DsbA reacts specifically with membrane-bound DsbB to form a mixed disulfide DsbA-DsbB complex* ***(d),*** *which results in reoxidation of DsbA and reduction of DsbB.*

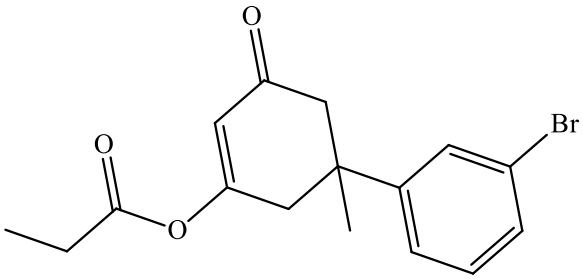

3'-bromo-1-methyl-5-oxo-1,2,5,6-tetrahydro-[1,1'-biphenyl]-3-yl propionate (**18**)

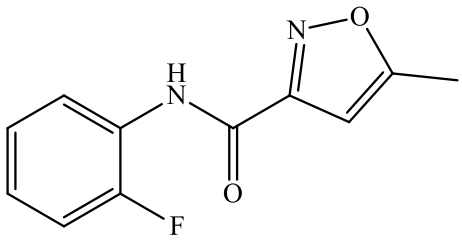

N-(2-fluorophenyl)-5-methylisoxazole-3-carboxamide (**19**)

Figure 3**:** Different molecule targeting *E.coli* DsbA enzyme

3.4. *In-silico* Studies

In-silico study has good predictive power to obtain perspective early stage of ADMET analysis. Even though there are a several of high-throughput in vitro models for ADMET profiling, in silico approaches are becoming increasingly popular due to their ability to make predictions quickly and affordably without requiring time-consuming and costly laboratory facilities (Daoud et al., 2021).

A computer tool based on structure, molecular docking determines the binding position and affinity between ligands and targets. To acquire a successful result, molecular docking requires meticulous adherence to certain protocol uses for molecular docking at distinct phases of drug discovery (Muhammed & Aki-Yalcin, 2022). This improves the prediction power in conjunction within silico ADMET technologies, as they are not precise on their own (Chang et al., 2023).

The preferred orientation of a ligand, when it binds to a particular receptor, which is typically a protein, to create a stable complex is predicted by molecular docking. The protein is the "lock", and the ligand is the "key", think of it as a "lock-and-key" problem. The objective is to determine the ligand's optimal orientation within the protein's binding site (Abdolmaleki et al., 2021).

4. MATERIALS AND METHODS

4.1. Materials

4.1.1. Chemicals and Reagents

The chemicals used are Methanol (99.6%), n-hexane (99.8%), Chloroform 99.8%), Diethyl ether (99.9%), ethanol (99.6%), bought from LOBA chemie Pvt.Ltd. and all are HPLC graded. Sulphuric acide, Benzoin, Urea, Formaldehyde, Peperidine, DMSO, (PBH), obtained from Addis Ababa University school of Pharmacy Pharmaceutical and Pharmacognosy lab.

4.1.2. Instruments

To perform the reaction, analysis and purification of the compounds different materials are used, such as analytical TLC plates (60-120 mesh Per-coated plastic Sheet POLYGRAM SIL G/UV_{254} with layer of 0.2mm thick Germany), for reaction monitoring and analytical, filter paper Watman No-1 (90mm), Water bath, Micro-pipette (10-200μl), Rota evaporator (Hiedolph Laborota 4001 efficient Germany), Vacuum pump V-700 (BHUCHI Labortechin AG Switzerland) for removal of the solvent, ARXE-Heat, reaction flask, and Magnetic stirrer, for the reaction, UV-Visible Spectrophotometry (UV-CAMAG), was used to visualize the TLC plates and electronic balance (SICENTHECH SA) for weighing amount of the chemicals.

NMR spectra were recorded using 400MHz for ^{1}H and 100MHz for ^{13}C NMR on a Bruker Advance DMX400 FT-NMR Spectrometry (Bruker Billerica Idaho, USA), tetramethyl silane (TMS) for the internal standard and detureted chloroform ($CDCl_3$) as a

solvent for the NMR Spectroscopy. Incubator (Model 100-800 memmert), autoclave, biosafety cabinet and inoculating loops are used for anti-microbial assay.

4.1.3. Media, Microbial Strains and Standard Drugs

Nutrient Agar (NA), Mueller-Hinton Broth (MHB), Sabouraud Dextrose Agar (SDA) and Sabouraud Dextrose Broth (SDB) from (HiMedia Laboratory Pvt. Ltd. India)

The bacterial strains *Bacillus subtilis* ATCC 6633, *Bacillus pumilus* 82, *Staphylococcus aureus* ML 267, *S. aureus* MDR1, and *S. aureus* MDR2 were all subjected to in vitro antibacterial tests. *E. Coli* 3:37C, *E. Coli* 7360, *E. Coli* 872, *E. Coli* CD/99/1, *E. Coli* K 88, *E. Coli* T 37, *E. Coli* ROW 7/12, *E. Coli* 5933, *E. Coli* HB101, *E. Coli* C600, *Salmonella enterica* TD 01, *Salmonella typhi* Ty2, *Shigella boydii* D13629, *Salmonella dysentery* 8, *Shigella flexneri* Type 6, *Shigella sonnei1*, *Vibrio cholerae* NCTC 5596, *V. cholerae* NCTC 10732, *Vibrio cholerae* NCTC 11501, *Vibrio cholerae* NCTC 4693, and *P. aeruginosa* MDR1 were among the Gram-negative bacterial strains utilized. The Central Drugs Laboratory in Kolkata, the Department of Technology at Jadavpur University, and the Institute of Microbial Technology in Chandigarh, India, where the sources of all the bacterial strains. The strains' purity was examined using the common microbiological, cultural, and biochemical assays prior to sensitivity testing on the test samples.

Conversely, the following organisms were tested for antifungal activity: *P. notatum* ATCC 11625, *Aspergillus niger* ATCC 6275, *Penicillium funiclosum* NCTC 287, and *Candida albicans* ATCC 10231. All the fungal species were provided from Central Drugs Laboratory, Kolkata Institute of Microbial Technology, Chandigarh, India.

Ciprofloxacin is an antibiotic belonging to the fluoroquinolone class used as standard drug for antibacterial test, whereas Griseofulvin standard drug for standard drug for antifungal test.

4.2. Methods

4.2.1. Synthesis of 2-Hydroxy-1, 2-diphenylethanone Derivatives

2-Hydroxy-1,2-diphenylethanone derivatives were synthesized via a one-pot, three-component Mannich reaction using benzoin, formaldehyde, and either a secondary amine (diethylamine or piperidine) or urea, resulting in the formation of 3-(diethylamino)-2-hydroxy-1,2-diphenylpropan-1-one (**20**), 1-(2-hydroxy-3-oxo-2,3-diphenylpropyl)urea (**21**), and 2-hydroxy-1,2-diphenyl-3-(piperidin-1-yl)propan-1-one (**22**), respectively.

4.2.1.1. Synthesis of 3-(diethylamino)-2-hydroxy-1,2 diphenylpropan-1-one) (20)

Initially, 0.83 g (4 mmol) of benzoin was placed in a 100 mL reaction flask, followed by the addition of 30 mL of methanol. The mixture was stirred at 50 °C using a magnetic stirrer until the benzoin fully dissolved. Subsequently, 0.85 ml of 37% solution of formaldehyde and four drops of concentrated sulfuric acid were added as a catalyst. In a separate beaker, 0.36 g (1.334 mmol) of diethylamine was dissolved in 20 mL of methanol. This solution was then added gradually to the reaction flask containing benzoin solution. The reaction mixture was then stirred at 80 °C with a stirring rate of 500 rpm. The progress of the reaction was monitored using TLC every 60 min for a total duration of 8 hrs. The reaction mixture was then transferred to a round-bottom flask, and the solvent was removed using a rotary evaporator at 80 °C until the product was completely dried. The dried product was subsequently collected and purified using flash column

chromatography, employing an increasing gradient of ethyl acetate in hexane as the eluting solvent.

4.2.1.2. Synthesis of 1-(2-hydroxy-3-oxo-2, 3-diphenylpropyl) urea (21)

Initially, 0.85 mL of a 37% formaldehyde solution was added to a 100 mL reaction flask, followed by the addition of 20 mL of methanol. Then, four drops of concentrated sulfuric acid were added as a catalyst. Next, 0.6 g of urea was added to the reaction flask containing the formaldehyde–sulfuric acid–methanol mixture. In a separate beaker, 4 mmol of benzoin was dissolved in 30 mL of methanol, and this solution was added to the reaction flask. The mixture was stirred at 50 °C, and the progress of the reaction was monitored using TLC every 60 min for a total of 20 hrs. The reaction mixture was then transferred to a round-bottom flask, and the solvent was removed using a rotary evaporator at 50 °C until the product was completely dried. The dried product was subsequently collected and purified using flash column chromatography.

4.2.1.3. Synthesized of 2-hydroxy-1, 2-diphenyl-3-(piperidin-1-yl) propan-1-one (22)

Compound **22** was synthesized by adding 0.68 mL of a 37% formaldehyde solution, 20 mL of methanol, and four drops of concentrated sulfuric acid into a 100 mL reaction flask. Next, 0.85 g (2 mL) of piperidine was added to the reaction flask. In a separate beaker, 4 mmol of benzoin was dissolved in 30 mL of methanol and then added to the reaction mixture. The mixture was stirred at 80 °C, and the progress of the reaction was monitored using TLC every 60 min over a 12 hrs period. The reaction product was transferred to a round-bottom flask, and the solvent was removed using a rotary evaporator at 80 °C until completely dry. The dried product was then collected and

purified by flash column chromatography using an increasing gradient of chloroform in hexane as the eluting solvent.

4.2.2. Structural Confirmation of the Synthesized Compounds

The structures of compounds **20, 21** and **22** were identified by analyzing their ^{1}H and ^{13}C-NMR spectra data. The chemical shifts are denoted in ppm and coupling constants (J) are expressed in Hz. Signal multiplicities are indicated as follows: *s* = singlet; *d* = doublet; *t* = triplet; *ddd* = doublet of doublet of doublets; and *m* = multiplet.

4.2.3. In vitro antimicrobial assay

4.2.3.1. Disk diffusion method

The disk diffusion method was used to screen the in vitro antibacterial assay by evaluating the zones of inhibition generated by the test samples. It is a time-consuming method that requires antimicrobial disk diffusion testing and interpretation (Daliri Shamsabadi, 2024; Jorgensen & Turnidge, 2015)

By making a stock solution of 1 mg/mL of the benzoin derivatives in 1% DMSO, the antibacterial and antifungal effects of the chemicals produced were investigated. The antibacterial and antifungal activity test values ranged from 5 to 800µg/mL for antibacterial and from 50 to 2000 µg/mL antifungal. Then the stock solution was diluted in the proper amounts of distilled water. After that, sterile Petri dishes were filled with molten media and incubated for 24 hours at 37 °C to check for contamination to create serial nutritional agar plates. After serial nutrient production, the inoculums were evenly swabbed and left to dry for five minutes. The Petri plates were subsequently incubated

for 24 hrs at 37 °C, and the diameter of the inhibitory zone was determined in millimeters. The experiment was performed using 1% DMSO as a negative control and ciprofloxacin as a positive control for bacteria. The Zone of inhibition (ZOI) was then compared with the standard drug (Patel et al., 2011). The ZOI test was reputed three times /3X/ and the ZOI was calculated based on mean of the three reputed experiment.

On Saborauds dextrose media, the test samples' antifungal potential was evaluated using an identical methodology against the fungal infections. Millimeters were used to measure the ZOI's diameter in the Petri plates following three days of room temperature incubation. Griseofulvin was used in this instance as the standard drug. The experiment was reputed three times /3X/ and the ZOI was calculated based on mean of the three reputed experiment.

4.2.3.2. Broth dilution method

The minimum inhibitory concentration (MIC) of the produced compounds was determined using broth dilution procedure (Steward et al., 2001). The Mueller–Hinton broth and Saborauds dextrose broth were used for bacterial growth and fungal, respectively. The produced compounds were dissolved in 1% DMSO at concentrations of 5, 10, 25, 50, 100, 200, 400, and 800µg/mL for the antibacterial activity test and 50, 100, 200, 400, 800, 1000, 1500, and 2000 µg/mL for the antifungal activity test.

A sterility control, which involves growth control using nutritious broth and DMSO devoid of antibiotics, was also carried out. Each test well and growth control well was cultured for three days at 25 °C for fungi and for twenty-four hours at 37 °C for bacteria. MIC was indicated by the test tubes' lack of turbidity (Wiegand et al., 2008).

4.2.4. *In* silico study

4.2.4.1. Molecular docking

A protein-ligand docking technique called CB-Dock automatically finds the binding sites, determines their size and center, and adjusts the docking box's dimensions based on the query ligands. The hit percentage and accuracy of blind docking can be improved by cavity-focused docking, according to extensive benchmarking. As a result, CB-Dock can speed up the docking process and increase accuracy by employing our curvature-based cavity detection method to forecast the target proteins' binding locations (Trott & Olson, 2010). CB-Dock workflow comprised six stages: Input and Preprocessing, Cavity Detection, Grid Generation, Docking Simulation with Autodock Vina, Score Ranking & Results Visualization and Output.

4.2.4.1.1. Input and Preprocessing

The ligand and protein structures, usually in the form of PDB files, provide the system. The system makes sure the protein file is in the right format for additional analysis and cleans up the structure (e.g., by eliminating water molecules or other heteroatoms) and making certain the file is in the appropriate format for additional examination (Liu & Cao, 2024).

4.2.4.1.2. Cavity Detection

CB-Dock uses a curvature-based approach to scan the protein's surface. By determining the geometric features especially, the curvature, size, and form of the surface depressions this finds possible binding pockets. Then, the server defines cavity parameters by

determining the size and center coordinates of each cavity it detects, which are then used to configure the docking grid boxes (Liu & Cao, 2024).

4.2.4.1.3. Grid Generation

A grid box is used to encapsulate each detected cavity. This box indicates the area of space where the ligand will dock throughout the simulation.

4.2.4.1.4. Docking Simulation with Autodock Vina

CB-Dock simulates the docking process using Autodock Vina for each grid box, or possible binding site by investigating binding modes using anticipated binding energies. Autodock Vina conducts a conformational search for the ligand, sampling several orientations and conformations to identify the ideal binding posture.

4.2.4.1.5. Scoring and Ranking

Assessment of binding affinities postures with corresponding scores (binding energies) are generated by every docking simulation. The rank for each cavity emphasizes the best candidates, which is typically the one with the lowest binding energy.

4.2.4.1.6. Results Visualization and Output

Interactive display of three-dimensional representation of the top binding positions within the protein structure is included in the final result. Downloadable data for additional documentation, data that include binding positions, scores, and cavity characteristics such center and size.

3.2.4.2. **Pharmacokinetics and drug-likeness properties**

With the aid of the online software tool ADMET lab 3.0, the physicochemical, pharmacokinetic, and toxicity characteristics of the produced compounds were anticipated (Dong et al., 2018). To facilitate this analysis, the compounds' structures were transformed into SMILES format using Chem Draw Ultra 12.0 software. The resulting SMILES of each compound were submitted as an input to the web server of ADMET lab 3.0.

There is growing pressure on the pharmaceutical sector to cut down on the time and money spent on finding and developing new medications. Consequently, advanced *in vitro* tests have been developed with the goal of simulating and forecasting the *in vivo* scenario. *In silico* techniques proved invaluable tools to help medicinal chemists to choose the most promising compounds for synthesis and to address the problem of managing the generated information (Riedel, 2013).

The web server's ADMETlab 3.0 offers a thorough and effective platform for assessing ADMET-related metrics, physicochemical features, and medicinal chemistry traits that are important to the drug discovery process (Fu et al., 2024).

5. RESULT AND DISCUSSION

5.1. Synthesis 2-Hydroxy-1, 2-diphenylethanone Derivatives

In this study, three compounds, 3-(diethylamino)-2-hydroxy-1,2-diphenylpropan-1-one (**20**), 1-(2-hydroxy-3-oxo-2,3-diphenylpropyl)urea (**21**), and 2-hydroxy-1,2-diphenyl-3-(piperidin-1-yl)propan-1-one (**22**), were successfully synthesized from 2-hydroxy-1,2-diphenylethanone using a one-pot reaction. The synthesis followed a Mannich-type reaction pathway, leading to the formation of β-amino alkylation products. The physical properties of these compounds are presented in Table 2.

Table 2: Physical properties of the synthesized compounds

Compound	MF	MW	Colour	PS	Yield	R_f *value*
20	$C_{19}H_{23}NO_2$	297.37	White	Crystal	56%	0.7
21	$C_{17}H_{17}NO_3$	283.32	White	Crystal	87%	0.4
22	$C_{20}H_{23}NO_2$	309.40	Yellowish	Powder	64%	0.8

Key: MF=Molecular formula, MW= Molecular weight, PS= Physical state, R_f = Retention factor

5.1.1. Synthesis of 3-(Diethylamino)-2-hydroxy-1,2-diphenylpropan-1-one (20)

3-(Diethylamino)-2-hydroxy-1,2-diphenylpropan-1-one (**20**) was synthesized as a white crystalline solid via a Mannich reaction using benzoin, formaldehyde, and diethylamine in the presence of an acid catalyst. In the presence of an acid catalyst, the reaction proceeds through a series of steps. Initially, formaldehyde is protonated by sulfuric acid (H_2SO_4), which increases its electrophilicity and makes it more susceptible to nucleophilic attack. Diethylamine then reacts with the protonated aldehyde to form an iminium ion intermediate. Meanwhile, benzoin undergoes enolization, also facilitated by

the acid catalyst, to generate an enol species. This enol acts as a nucleophile and attacks the electrophilic iminium ion, resulting in the formation of a new carbon–carbon bond. Finally, deprotonation and rearrangement yield the *β*-amino carbonyl product, 3-(diethylamino)-2-hydroxy-1,2-diphenylpropan-1-one (**20**). The reaction mechanism for compound **20** illustrated schem 1 below.

Reaction mechanism for the synthesized compound **20**

Step-1 Formation of the Iminium Intermediate:

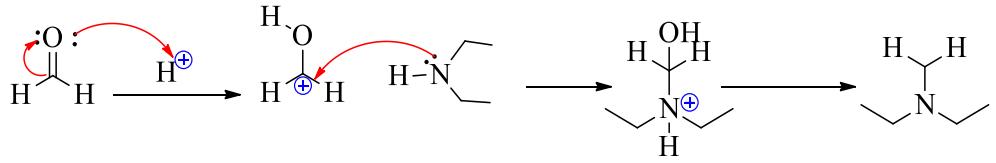

Step-2 Generation of the Nucleophilic Species

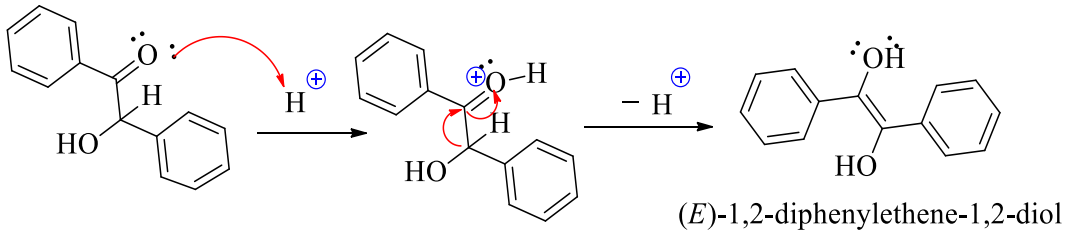

Step-3 Nucleophilic Addition

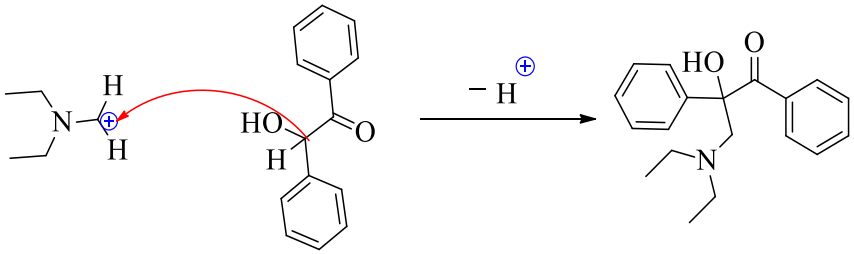

Scheme 1: The reaction mechanism of 3-(diethylamino)-2-hydroxy-1, 2-diphenylpropan-1-one (**20**)

5.1.2. Synthesis of 1-(2-Hydroxy-3-oxo-2,3-diphenylpropyl)urea (21)

1-(2-Hydroxy-3-oxo-2,3-diphenylpropyl)urea (**21**), was synthesized as a white crystalline through Mannich reaction following the some synthesis procedure outlined for compound

20, unless substitution of urea for diethylamine. The reaction mechanism for compound **21** closely resembles that of compound **20,** and illustrated in scheme 2 below.

Reaction mechanism for the synthesized compound **21**

Reaction mechanisum

Step-1 protonation of the formaldehyde form of the carbocvtion

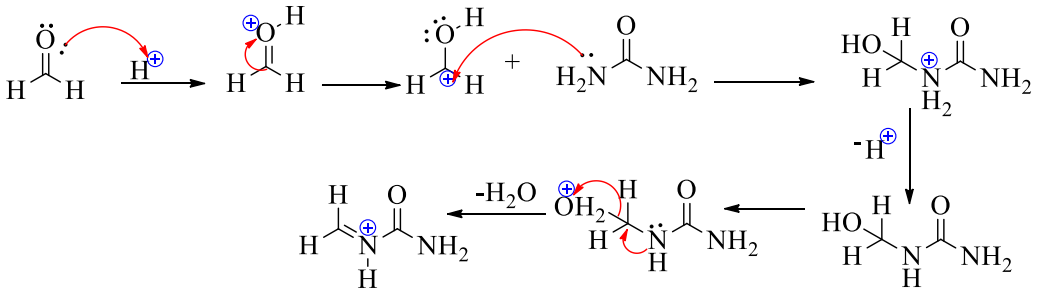

Step-2 The ketone which have alpha hydrogen is protonated and deprotonated to tautomeris to get enole intermidet

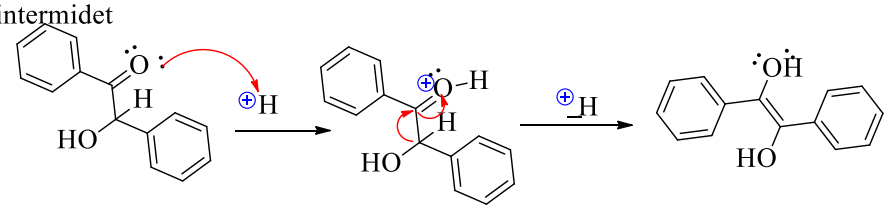

Step-3 The intermidate inole attacks the iminium ion and after deprotonotion forms a beta amino-keton which is the mannick product

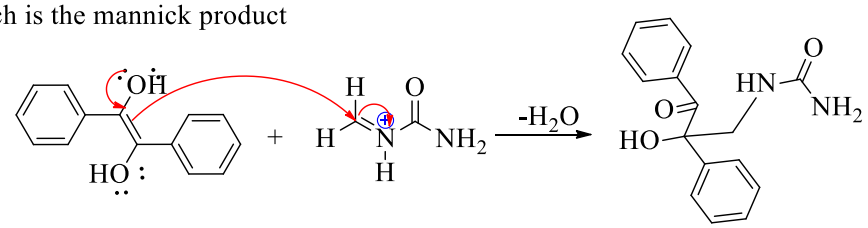

Scheme 2: Reaction mechanism in the Synthesis of 1-(2-hydroxy-3-oxo-2, 3- **(21)**

5.1.3. Synthesis of 2-Hydroxy-1,2-diphenyl-3-(piperidin-1-yl)propan-1-one (22)

2-Hydroxy-1,2-diphenyl-3-(piperidin-1-yl)propan-1-one (**22**) was synthesized as a yellowish powder via the some synthesis procedure outlined for compound **20**, unless substitution of piperidine for diethylamine. The reaction mechanism for compound **22** illustrated in scheme 3 below.

Reaction mechanism for the synthesized compound **22**

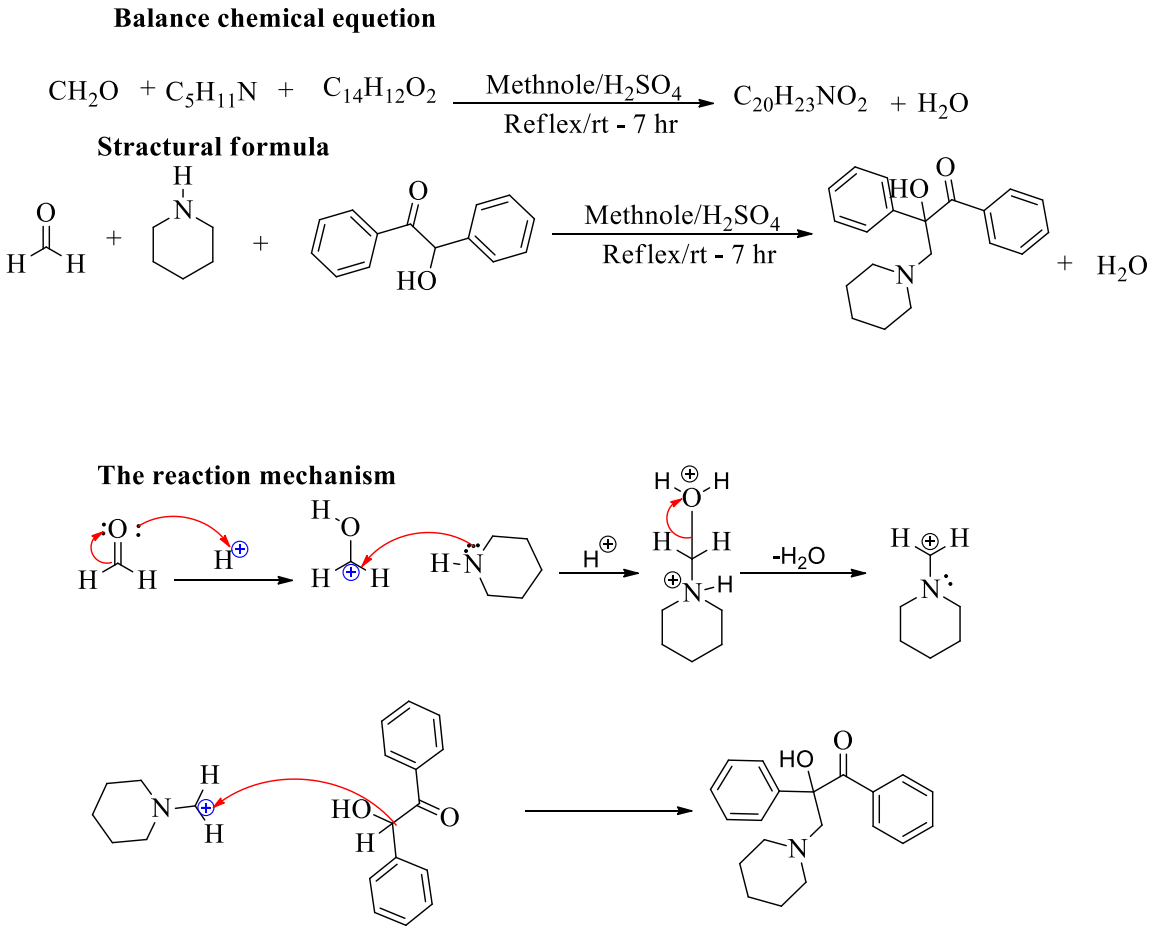

Scheme 3: Reaction mechanism in the Synthesized of 2-hydroxy-1, 2-diphenyl-3-(piperidin-1-yl) propan-1-one (**22**).

5.2. Structural Confirmation of 2-Hydroxy-1, 2-diphenylethanone Derivatives

The successful synthesis of compounds **20**, **21**, and **22** was confirmed through detailed analysis of their ^{1}H and ^{13}C-NMR spectral data. Compound **20** was identified as 3-(diethylamino)-2-hydroxy-1,2-diphenylpropan-1-one, compound **21** as 1-(2-hydroxy-3-oxo-2,3-diphenylpropyl)urea, and compound **22** as 2-hydroxy-1,2-diphenyl-3-(piperidin-1-yl)propan-1-one.

The chemical shifts in the NMR spectra were consistent with the proposed structures of each compound, thereby confirming the successful formation and structural integrity of the synthesized products.

5.2.1. Structural Confirmation of Compound 20

Compound **20** was synthesized as white crystalline solid with an R_f value of 0.7 on TLC using a hexane/chloroform (2:1) solvent system as the mobile phase. The ^{1}H and ^{13}C-NMR spectral data for compound **20** revealed the presence of characteristic functional groups and structural features consistent with a substituted aromatic ketone bearing aliphatic and phenolic components. The ^{1}H-NMR spectrum displayed a triplet at δ 1.24 ppm (3H, *J*=6.7 Hz, H-1) and a quartet at δ 2.96 ppm (2H, *J*=6.8 Hz, H-2), consistent with an ethyl group (–CH_2CH_3) moiety. A pair of doublets at δ 3.00 and 3.08 ppm (H-3) suggested diastereotopic methylene protons adjacent to an electronegative group or stereocenter. A singlet at δ 6.00 ppm corresponded to a hydroxyl (OH) proton, indicating the presence of a free phenolic or alcoholic group. Aromatic proton signals appeared as multiplets and doublets in the region δ 7.40–7.94 ppm, characteristic of substituted aromatic rings. Specifically, protons H-2', H-3', H-3", and H-4" resonated within δ 7.40–7.94 ppm, suggesting two distinct aromatic systems with overlapping.

The ^{13}C-NMR spectrum further supported these structural features. The aliphatic carbon atoms appeared at δ 11.01 (C-1), 41.73 (C-2), and 50.95 (C-3), corresponding to the ethyl and methylene carbons. A downfield resonance at δ 77.44 (C-4) was indicative of a carbon bearing a hydroxyl group.

The signal at δ 194.6 (C-5) confirmed the presence of a carbonyl carbon, a ketone. The aromatic carbons (C-1' to C-4' and C-1" to C4") appeared in the δ 124.02–141.07 ppm range, consistent with substituted benzene rings. Detailed ^{1}H and ^{13}C-NMR chemical shifts were presented in Table 3. Finally, compound **20** was unambiguously characterized as 3-(diethylamino)-2-hydroxy-1,2-diphenylpropan-1-one.

Table 3: ^{1}H and ^{13}C-NMR spectral data of compound **21**

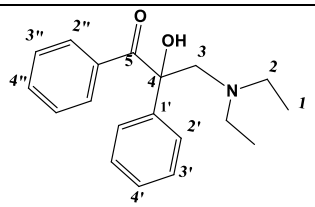

	^{1}H -NMR δ (ppm)		**^{13}C-NMR δ (ppm)**
H-1	1.24 (6H, *t*)	C-1	11.01
H-2	2.96 (2H, *q*)	C-2	41.73
H-3	3.00, 3.08 (2H, *d*)	C-3	50.95
OH	6.00 (1H, *s*)	C-4	77.44
		C-5	194.6
H-2'- H-4'	7.51-7.52 (5H, *m*)	C-1'-C-4'	124.02-141.07
H-2"	7.94 (2H, *d*)	C1"-C-4"	124.02-141.07
H-3"	7.40 (2H, *m*)		
H-4"	7.52 (1H, *m*)		

Key: *d = doublet, m = multiplet, q = qu*artat, *s = singlet, t = triplet*

The ^{13}C-NMR (126 MHz, $CDCl_3$) demonstrates the presences of two methyl groups C-1 (δ=11.01), the presence of methylene carbon C-2&3 ((δ=41.73 & 50.93), also quaternary carbon at (δ=77.44) and aromatic carbons. (See table 2 and annex). Thus, the structure of compound **20** was confirmed by both ^{1}H-NMR and ^{13}C-NMR investigations. Table 4 displays the precise chemical shifts for each of the other protons and carbons in compound **20**.

5.2.2. Structural Confirmation of Compound (21)

Compound **21** was successfully synthesized as a white crystal with an R_f value of 0.6 on TLC using Hexane/Chlorform (2:1) as the mobile phase. The ^{1}H and ^{13}C-NMR spectral data of compound **21** displayed a structure featuring both aliphatic and aromatic components, along with amine and carbonyl functionalities. In the ^{1}H-NMR spectrum, a doublet at δ 4.1 ppm (H-1) and a corresponding carbon (C-1) appeared at δ 55.23 ppm in the ^{13}C-NMR spectrum, consistent with a methylene carbon next –NH– group. In addition, a carbon signals appeared at δ 78.23 ppm, represented an oxygenated carbon (C-2), potentially part of a tertiary alcohol. Further analysis of the ^{1}H-NMR spectrum showed singlets at δ 6.0 ppm corresponding to both an –NH– and an –NH₂ group, along with the associated carbon C-3 at δ 167.32. These signals were likely part of a urea or amide-type moiety. In addition, a carbon signal resonated at δ 197.78 ppm, indicating the presence of carbonyl carbons, typical of ketone (C-4).

The aromatic region in the ^{1}H-NMR spectrum includds multiplets between δ 7.2–7.6 ppm (H-2′–H-4′) and δ 7.7–8.0 ppm (H-2″–H-4″), indicative of two distinct aromatic systems. These were supported by the ^{13}C-NMR signals ranging from δ 122.00–138.67 ppm for C-1′–C-4′ and δ 120.0–139.2 ppm for C-1″–C-4″, consistent with substituted benzene rings. Table 4 displays the all chemical shifts for each of the protons and carbons in compound **21**. At the end, compound **21** was identified as 1-(2-hydroxy-3-oxo-2,3-diphenylpropyl)urea, based on the ^{1}H and ^{13}C-NMR spectral data.

Table 4: ^{1}H and ^{13}C-NMR spectral data of compound **21**

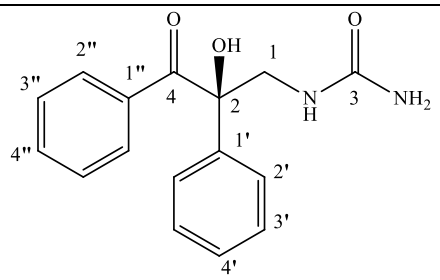

	^{1}H-NMR δ (ppm)		^{13}C-NMR δ (ppm)
H-1	3.9, 4.1 (2H, *d*)	C-1	55.23
-OH	4.1 (1H, *s*)	C-2	78.23
-NH-	6.0 (1H, *s*)	C-3	167.32
-NH_2	6.0 (2H, *s*)	C-4	197.78
H-2'- 4'	7.2 – 7.6 (5H, *m*)	C-1'- 4'	122.00-138..67
H-2" - 4"	7.7 – 8.0 (5H, *m*)	C-1" - 4"	120.139.2

Key: *d = doublet, m = multiplet, s = singlet,*

5.2.3. Structural Confirmation of Compound 22

Compound **22** was synthesized as a yellowish powder (M.wt 309) with an R_f value of 0.8 on TLC using Hexane/Chloroform (2:1) as the mobile phase. The ^{1}H and ^{13}C-NMR spectral data of compound **22** suggested a molecular structure incorporating aliphatic chains, hydroxyl and amine functionalities, and two aromatic rings. In the aliphatic region of the ^{1}H-NMR, a broad multiplet between δ 1.13–1.59 ppm (H-1 & H-2) corresponded to methylene protons, whose associated carbons appeared in the ^{13}C-NMR spectrum at δ 21.30–22.17 ppm, indicating typical saturated carbon environments. A triplet at δ 2.64 ppm (H-3) and a pair of doublets at δ 2.65 and 2.46 ppm (H-4) were indicative of methylene groups adjacent to electronegative atoms (nitrogen). These protons corresponded to carbons resonating at δ 53.90 ppm (C-3, C-4), suggesting significant deshielding due to nearby nitrogen atom.

The singlet at δ 3.74 ppm was assigned to a hydroxyl proton, implying the presence of a free –OH group on one of the aliphatic carbons. The signal at δ 53.90 ppm chemical shift value for C-3 to C-4 supported a set of closely related or symmetrical carbon environments, possibly within a branched or cyclized amine system. In the aromatic region, two sets of multiplets spanning δ 7.11–8.12 ppm (H2′–H4′ and H2″–H4″) indicated the presence of two substituted benzene rings. The corresponding aromatic carbons resonated in the ^{13}C-NMR at δ 123.00–127.32 ppm (C1′–C4′) and δ 126.78–138.96 ppm (C1″–C4″), confirming two distinct aromatic systems with slightly different electronic environments, likely due to substitution patterns or adjacent functional groups. Detailed 1H and 13C-NMR chemical shift are provided in Table 5. Overall, compound **22** was identified as 2-hydroxy-1,2-diphenyl-3-(piperidin-1-yl)propan-1-one.

Table 5: ^{1}H and ^{13}C-NMR spectral data of compound **22**

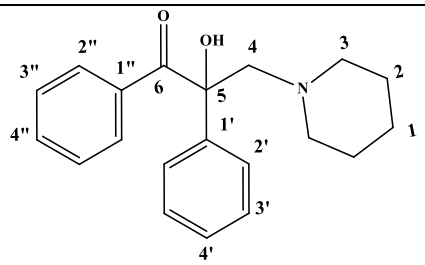

	^{1}H-NMR δ (ppm)		**^{13}C-NMR δ (ppm)**
H-1& H-2	1.13-1.59 (5H, *m*)	C-1&2	21.30-22.17
H-3	2.64 (4H, *t*)	C-3	53.90
H-4	2.65, 2.46 (2H, *d*)	C-4	62.70
OH	3.74 (1H, *s*)	C-5	80.01
		C-6	198.20
H-2'-4'	7.11-8.12 (5H, *m*)	C-1'-4'	123.00-127.32
H-2"-4"	7.11-8.12 (5H, *m*)	C-1"-4"	126.78-138.96

Key: *d = doublet, m = multiplet, q = qu*artat*, s = singlet, t = triplet*

5.3. Antimicrobial Activity of the Synthesized Compound

5.3.1. Antibacterial Activity

In this study, the antibacterial activity of 2-hydroxy-1,2-diphenylethanone derivatives **20**, **21**, and **22** was evaluated against 26 bacterial strains using both the disc diffusion and broth dilution methods. The results are summarized in Table 7, showing ZOIs ranging from 6.0 to 15.8 mm and MICs ranging from 10µg/mL to 800µg/mL. Among the three compounds, compound **21** exhibited the strongest antibacterial activity, particularly against *Shigella sonnei* 1 and *Shigella boydii* D13629, with a ZOI of 15.8 mm and an MIC of 10µg/mL. These results highlight the significance of compound **21**, as both *S. sonnei* and *S. boydii* are important human-adapted pathogens contributing to the global burden of diarrheal disease. The genus *Shigella* remains a major public health concern due to the increasing prevalence of antibiotic-resistant strains, the lack of an effective vaccine, and various environmental factors (Miles et al., 2024; Scott et al., 2024; McQuade et al., 2025).

Pseudomonas aeruginosa is associated with high morbidity and mortality rates, particularly due to its role in severe hospital-acquired infections such as ventilator-associated pneumonia and sepsis. The global emergence of antimicrobial-resistant *P. aeruginosa* strains has significantly complicated treatment efforts, largely due to the decreasing effectiveness of available therapeutic options (Salleh et al., 2025).

Notably, compound **21** also exhibited strong antibacterial activity against the multidrug-resistant strain *P. aeruginosa* MDR1, with a ZOI of 14.8 mm and a MIC of 10 µg/mL. However, compound **21** was the least effective against *Bacillus pumilus* 82 and *Bacillus subtilis* ATCC 6633, which are known to cause opportunistic infections such as

bacteremia, endocarditis, and foodborne illnesses. Against these strains, compound **21** showed a ZOI of only 6.0 mm and a MIC of 400 µg/Ml.

Compounds **20** and **22** showed strong activity against multiple *E. coli* strains, each with a MIC of 25 µg/mL. *E. coli* is linked to a wide range of diseases, including urinary tract infections, gastroenteritis, neonatal meningitis, and sepsis, and is responsible for the deaths of approximately 2.9 t0 10.3 deaths per 100,000 persons-year worldwide annually (MacKinnon et al., 2021).

In summary, the synthesized compounds demonstrated broad-spectrum antibacterial activity against a wide range of bacterial strains, including both Gram-positive and Gram-negative species. This is particularly noteworthy given that most existing antibiotics are narrow-spectrum, targeting only specific types of bacteria. Therefore, these compounds hold significant potential as therapeutic agents in the treatment of polyinfectious diseases, where infections are caused by multiple bacterial species simultaneously.

Table 6: Zone of inhibition and minimum inhibitory concentration of synthesized compounds against the tested bacterial strains.

	ZOI in mm (200µg/ml)				**MIC (µg/ml)**		
Bacteria strain	**20**	**21**	**22**	Ciprofloxacin	**20**	**21**	**22**
E.coli K99	13.5	12.2	13.5	16.0	25	100	25
E.coli K88	14.8	12.5	14.8	17.0	25	100	25
E.coli 306	14.0	13.0	14.3	17.0	25	100	25
E.coli LT37	14.0	12.5	14.0	16.0	25	100	25
E.coli 872	14.5	12.7	14.5	15.8	25	100	25
E.coli ROW 7/12	15.0	12.0	14.5	16.5	25	100	25
E.coli 3:37C	15.2	11.8	15.2	16.5	25	100	25
E.coli CD/99/1	15.7	12.2	15.7	16.8	25	100	25
Salmonella typhi Ty2	13.2	13.7	11.8	16.0	400	100	800

Salmonella enterica TD 01	14.2	14.0	12.7	19.0	400	100	800
Shigella dysentery 8	13.8	13.7	13.8	20.0	100	100	100
Shigella soneii 1	14.0	15.8	14.0	19.5	50	10	50
Shigella boydii D13629	14.0	15.8	14.0	20.0	50	10	50
Shigella flexneri Type 6	15.8	15.5	15.8	20.5	50	50	50
Staphylococcus aureus MDR10	14.3	14.7	14.3	18.0	100	400	100
Bacillus pumilus 82	9.0	6.0	8.0	18.8	200	400	800
Bacillus subtilis ATCC 6633	10.2	6.0	7.5	18.0	200	400	800
Vibrio cholerae 1313	12.0	13.3	12.0	17.5	100	25	100
Vibrio cholerae 293	12.3	14.7	12.3	18.7	100	25	100
Vibrio cholerae 1315	11.3	14.8	11.3	19.0	100	25	100
Vibrio cholerae 85	11.2	14.0	11.5	18.5	100	25	100
*E.coli HB101**	13.2	14.0	12.2	16.0	200	25	100
*E.coli C600**	13.0	13.8	12.8	16.0	200	25	100
*S.aureus MDR 1**	14.2	14.2	14.3	18.0	100	25	100
*S.aureus MDR 2**	14.3	14.7	14.3	18.0	100	25	100
*Pseudomonas aeruginosa MDR 1**	14.0	14.8	13.0	17.3	200	10	50

Key: *ZOI = Zone of Inhibition, MIC = Minimum Inhibitory Concentration*
N.B Size of the disk = 6mm

5.3.2. Antifungal Activity

The synthesized compounds **20**, **21**, and **22** were also evaluated for their antifungal activity against four fungal strains using both the disc diffusion and broth dilution methods. As summarized in Table 7, all three compounds exhibited antifungal activity, with ZOIs ranging from 12.0 to 15.0 mm and MICs between 200 and 1000 µg/mL. One of the tested strains, *Penicillium funiculosum* NCTC 287, is known to cause rare opportunistic infections in humans, particularly in immunocompromised individuals. Interestingly, compound **22** showed the highest activity against *P. funiculosum*, with a

ZOI of 15.0 mm surpassing the standard antifungal agent griseofulvin, which had a ZOI of 14.0 mm.

Aspergillus species are capable of causing a broad spectrum of diseases, ranging from invasive infections to chronic pulmonary disorders and allergic syndromes. Among these, invasive *Aspergillosis* is one of the leading causes of morbidity and mortality in immunocompromised individuals, such as organ transplant recipients, cancer patients undergoing chemotherapy, and those with advanced HIV/AIDS (Cadena et al., 2021).

In this study, compound **22** demonstrated significant antifungal activity against *Aspergillus niger* ATCC 6275, with a ZOI measuring 15.0 mm and a MIC of 200 µg/mL. These results suggest that compound **22** may serve as a promising candidate for further development as an antifungal agent, particularly against pathogenic *Aspergillus* species.

Table 7: Zone inhibition and minimum inhibitory concentration of Synthesized compound against the tested fungal species.

	ZOI (2000 µg/ml)				**MIC (µg/ml)**		
Fungi	**20**	**21**	**22**	**Griseofulvin**	**20**	**21**	**22**
Candida albicans ATCC 10231	12.0	12.5	15.0	16.0	1000	1000	200
Aspergillus niger ATCC 6275	13.0	14.0	15.0	15.0	400	800	200
Penicillium notatum ATCC 11625	13.5	14.5	15.0	15.0	800	800	200
Penicillium funiculosum NCTC 287	13.0	12.5	15.0	14.0	800	800	200

Key: *ZOI = Zone of Inhibition, MIC = Minimum Inhibitory Concentration*
N.B Size of the disk = 6mm

5.4. *In silico* Studies

5.4.1. Molecular Docking

The synthesized compounds were evaluated for their potential inhibitory activity against the *E. coli* disulfide bond-forming protein A (DsbA) enzyme through molecular docking studies. For this purpose, the crystal structure of *E. coli* DsbA in complex with N-(2-fluorophenyl)-5-methylisoxazole-3-carboxamide, obtained from the Protein Data Bank (PDB ID: 8DN0) (Borrell et al., 2023) was utilized as the docking model. This structure provided a reliable template for assessing the binding affinity and interaction modes of the synthetic compounds within the enzyme's active site.

The molecular docking was conducted to analyze how well the compounds fit into the binding pocket and to identify key molecular interactions. The results revealed that several of the synthesized compounds exhibited favorable docking scores and formed stable interactions with critical active site residues, indicating their potential as promising DsbA enzyme inhibitors.

Among the tested compounds, compound **21** exhibited the most favorable docking score –7.5 kcal/mol, indicating the strongest predicted binding affinity to the *E. coli* DsbA enzyme relative to other synthesized compounds. Compound **22** followed with a docking score –7.1 kcal/mol, while compound **20** demonstrated a slightly lower score of –6.5 kcal/mol. These results, illustrated in ANNIX-III (Figures 3 to 5), suggest that the synthesized compounds have a good potential to interact effectively with the *E. coli* DsbA active site.

The molecular docking analysis further revealed that the compounds established multiple stabilizing interactions within the binding pocket. These included π-π stacking with key amino acid residues such as HIS32, GLN35, PHE36, LEU40, VAL150, PRO151, ALA152, LEU161, ASN162, PRO163, GLN164, GLY165, MET166, THR168, MET171, and PHE174. Additionally, several hydrogen bonds were formed involving oxygen and nitrogen atoms of the ligands, which further contributed to their stable accommodation within the active site of the enzyme. Overall, these findings support the potential of compounds **20**, **21**, and **22** as promising inhibitors of *E. coli* DsbA.

Table 8: Molecular Docking result of the synthesized compounds

Compound	**Cavity size(Angstrom cubed (Å³)**	**Docking score (kcal/mol)**	**Interaction with amino acid residues**	
			H-bonds	**Hydrophobic**
19	926	-6.7	HIS32,	PHE36
20	>>	-6.5	HIS32,	PHE36
21	>>	-7.5	HIS32, PHE36, THR161, PRO163	PHE174, LEU40,
22	>>	-7.1	HIS32, THR168	PHE174

Figure 4: Compound **20** complexes with E. coli DsbA

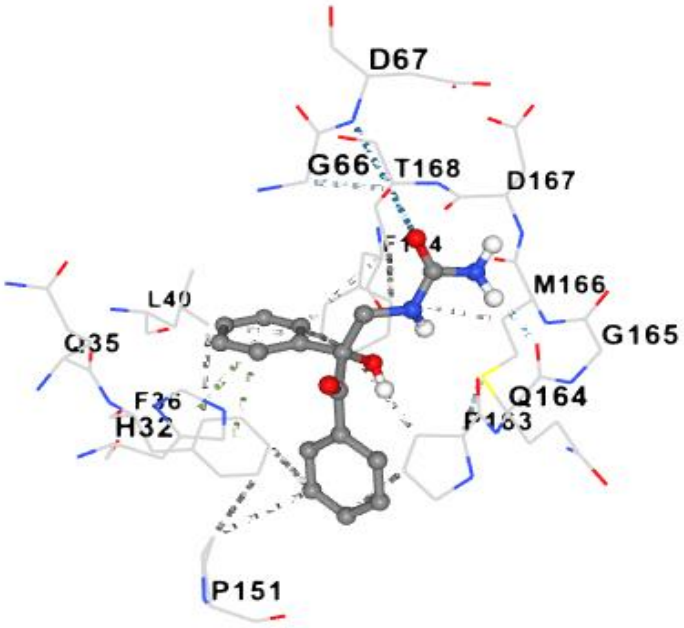

5.4.2. Pharmacokinetics and drug-likeness properties

The findings of this study showed that all three compounds demonstrated good intestinal absorption, volume of distribution, and plasma protein binding, which are important for their therapeutic effectiveness. However, all three exhibited low blood-brain barrier (BBB) permeability, making them less suitable for treating meningeal infections, as predicted by the ADMETlab 3.0 software (Table 9).

All three compounds were found to be non-inhibitors of CYP enzymes. However, compound **22** is a substrate of P-glycoprotein (P-gp), suggesting it may be actively effluxed from cells. Compounds **21** and **22** showed poor clearance profiles. Additionally, compounds **20** and **22** pose a potential risk of hERG (human ether-à-go-go-related gene) toxicity, which could lead to cardiac arrhythmias (Garrido et al., 2020). For detailed information see table 10 and 11 below.

We evaluated and contrasted all compounds' drug-likeness using Lipinski's rule of five. Lipinski's rule of five, which states that a molecule must have a molecular weight (MW) of less than 500, a logP (partition coefficient) of less than 5, hydrogen bond donors of less than 5, and hydrogen bond acceptors of less than 10, was met by three of the synthesized compounds. The synthesized compounds are expected to follow Lipinski's rule of five. Lipinski's rule of five is a set of criteria used to evaluate the drug-likeness of compounds, focusing on their absorption and permeation characteristics. Adhering to these guidelines can enhance the likelihood of successful drug development and bioavailability in pharmaceutical applications.

Moreover, we evaluated the synthetic compounds' toxicities, paying attention to cardiotoxicity, mutagenicity, and drug-induced liver damage. Both acute and chronic liver illnesses are known to result from drug-induced liver damage, which is particularly brought on by drugs. Three of the produced chemicals were anticipated to have negative effects on the liver, according to the data. Compound **21** showed toxicity in the Ames test for mutagenicity. Two compounds **20** and **22** were shown to be inhibitors when we examined their ability to block potassium channels encoded by hERG (human ether-a-go-go-related gene), a major contributing factor to the development of deadly ventricular arrhythmias.

Table 9: Pharmacokinetics profile prediction of synthesized compounds using ADMETlab 3.0 software

Compound	Caco-2 (Log unite)	Pgp-inhib	HIA	PPB (%)	VD (L/Kg)	BBB-Penet	CYP450 inhibition					Excretion	
							1A2	2C19	2C9	2D6	3A4	CL	$t_{1/2\ (hr)}$
20	-4.581	0.027	0.006	74.92	2.496	0.850	0.624	0.906	0.025	0.941	0.697	7.82	0.08
21	-5.219	0.042	0.202	71.23	0.734	0.996	0.636	0.539	0.145	0.215	0.310	2.088	0.194
22	-4.692	0.896	0.015	81.14	3.695	0.875	0.274	0.142	0.038	0.636	0.086	3.556	0.043
Optimal Value	>-5.00	0-0.3	0-0.3	<90%	0,04-20	0-0.3	0-1	0-1	0-1	0-1	0-1	>=5	0-0.3

Key: *Caco-2 = human colon adenocarcinoma cell lines, Pgp-inhib = P-glycoprotein inhibitor, HIA=Human intestinal absorption; PPB=plasma protein binding; BBB = blood–brain barrier, VD = Volume of distribution; CYP450=cytochrome P450, CL = clearance of a drug; t½= half-life;*

Table 10: Physicochemical Property & Toxicity profile prediction of compounds synthesized using ADMETlab 3.0 software

	nHA	nHD	NRot	TPSA	logS	LogP	LogD	SC	hERG	AMES	H-HT	Carcinogene
20	3	1	7	40.54	-3.934	3.173	3.214	1	0.351	0.049	0.051	0.019
21	5	4	6	92.42	-3.133	1.599	1.95	1	0.12	0.151	0.079	0.018
22	3	1	5	40.54	-4.199	3.401	3.39	1	0.62	0,053	0.064	0.034
Optimal Value	0-12	0-7	0-11	0-140	-4 to 0.5 log mol/L	0 to 3 log mol/L	1 to 3 log mol/L	<=2	0-0.3	0-0.3	0-0.3	0-0.3

Key: *nHA= number of hydrogen bond acceptors, nHD= number of hydrogen bond donors, nRot= number of rotatable bonds, TPSA=topological polar surface area, Log P = partition coefficient, LogS = aqueous solubility, LogD=n-octanol/water distribution coefficients at pH=7.4, SC= Stereo center, hERG = human ether-a-go-go related gene,; AMES = a test for mutagenicity; H-HT= human hepatotoxicity*

Table 11: Medicinal Chemistry profile prediction of compounds synthesized using ADMETlab 3.0 software

Compound	QED	Fsp3	SAscore	LR-5	Golden Triangle	PAINS
20	0.798	0.316	2.593	Accepted	Accepted	0 alerts
21	0.725	0.125	2.65	Accepted	Accepted	0 alerts
22	0.862	0.35	2.55	Accepted	Accepted	0 alerts
Optimal Value	≥ 0.67	≥ 0.42	≤ 6	< 2 violations	0 - violations	0

Key: *QED=measure of drug-likeness, SA score=synthetic accessibility score, LR-5=Lipinski rule of 5, Fsp^3 = number of sp3 hybridized carbons, PAINS = Pan Assay Interference Compounds*

6. CONCLUSION

This study successfully synthesized three novel derivatives of 2-hydroxy-1,2-diphenylethanone, all of which exhibited broad-spectrum antibacterial and antifungal activities. The synthesized compounds demonstrated significant antibacterial effects against a wide range of bacterial strains, including both Gram-positive and Gram-negative species, as well as multidrug-resistant strains. This broad-spectrum efficacy is particularly interesting, given that many existing antibiotics are limited in scope and target only specific bacterial types. As such, these compounds show strong potential as therapeutic candidates for the treatment of polyinfectious diseases. Compound **21** exhibited the most potent antibacterial activity, particularly against *Pseudomonas aeruginosa* MDR1, *Shigella sonnei* 1, and *Shigella boydii* D13629, with a MIC of 10 µg/mL. Compound **22** showed the highest antifungal activity, producing a ZOI of 15.0 mm against *Penicillium funiculosum* NCTC 287 surpassing the standard antifungal agent Griseofulvin, which had a ZOI of 14.0 mm.

Furthermore, molecular docking studies revealed that the synthesized compounds formed favorable interactions with the active site of the *E. coli* DsbA enzyme, which plays a crucial role in bacterial protein folding and biosynthesis. In conclusion, the 2-hydroxy-1,2-diphenylethanone derivatives developed in this study represent promising lead compounds for the development of new antimicrobial agents.

.

7. RECOMMENDATION

The current work recommends the following actions:

- ✓ Verify the molecular docking results experimentally.
- ✓ Produce more 2-hydroxy-1, 2-diphenylethanone and assess its possible antibacterial properties.
- ✓ Examine further possible biological activities for the three produced 2-hydroxy-1, 2-diphenylethanone molecules, such as antiviral, anticancer, anti-inflammatory, and antioxidant properties.
- ✓ Evaluate the safety profile of the produced chemicals, conduct thorough toxicity tests.

REFERENCES

Abdolmaleki, A., Shiri, F., & Ghasemi, J. B. (**2021**). Use of Molecular Docking as a Decision-Making Tool in Drug Discovery. *Molecular Docking for Computer-Aided Drug Design: Fundamentals, Techniques, Resources and Applications*, 229–243.

Asmare, Z., Tamrat, E., Erkihun, M., Endalamaw, K., Alelign, D., Getie, M., Sisay, A., Gashaw, Y., & Reta, M. A. (**2025**). Antimicrobial resistance pattern of Acinetobacter baumannii clinical isolate in Ethiopia. A systematic review and meta-analysis. *BMC Infectious Diseases*, *25*(1), 518.

Atia Sharif, H. N., Rehman, R., Mushtaq, A., & Rashid, U. A. (**2016**). Review on bioactive potential of Benzoin resin. *Int. J. Chem. Biochem. Sci*, *10*, 106–110.

B., W. G. . H. (2023). *E.coli DsbA in complex with N-(2-fluorophenyl)-5-methylisoxazole-3-carboxamide*.

Babu Kothapalli, R., Anusha, B., Naveen Kumar, M., Singh, P. S., Ramakrishna, S., & Venkata Subba Reddy, U. (**2025**). Deracemization of Benzoin and its Derivatives via Kinetic, Dynamic Kinetic, Aerobic Oxidative Kinetic, and Reagent-mediated resolution. *Chemistry–An Asian Journal*, e202401693.

Berkelman, R. L., Bryan, R. T., Osterholm, M. T., LeDuc, J. W., & Hughes, J. M. (**1994**). Infectious Disease Surveillance: a Crumbling Foundation. *Science*, *264*(5157), 368–370.

Blicke, F. F. (1942). The Mannich Reaction. *Organic Reactions*, *1*, 303–341.

Bongomin, F., Gago, S., Oladele, R. O., & Denning, D. W. (**2017**). Global and multi-national prevalence of fungal diseases—estimate precision. *Journal of Fungi*, *3*(4), 57.

Buran, K. (**2025**). Metal complexes of sulfamethazine/benzoin-based Schiff base ligand: synthesis, characterization, DFT calculations, and antimicrobial activities. *Turkish Journal of Biology*, *49*(SI-1), 118–126.

Cadena, J., Thompson, G. R., & Patterson, T. F. (**2021**). Aspergillosis: epidemiology, diagnosis, and treatment. *Infectious Disease Clinics*, *35*(2), 415–434.

Chang, Y., Hawkins, B. A., Du, J. J., Groundwater, P. W., Hibbs, D. E., & Lai, F. (**2023**). A Guide to In Silico Drug Design. In *Pharmaceutics* (Vol. 15, Issue 1).

Chen, W. (**2024**). The Role and Research Progress of Drug-Resistant Oral Microorganisms in the Pathogenesis of Periodontitis. *International Journal of Public Health and Medical Research*, *1*(2), 60–69.

Daliri Shamsabadi, O. (**2024**). Investigation of Antimicrobial Effect and Mechanical Properties of Modified Starch Films, Cellulose Nanofibers, and Citrus Essential Oils by Disk Diffusion Method. *Asian Journal of Green Chemistry*, *8*(1), 1–14.

Daoud, N. E.-H., Borah, P., Deb, P. K., Venugopala, K. N., Hourani, W., Alzweiri, M.,

Bardaweel, S. K., & Tiwari, V. (**2021**). ADMET Profiling in Drug Discovery and Development: Perspectives of In Silico, In Vitro and Integrated Approaches. *Current Drug Metabolism*, *22*(7), 503–522.

Denning, D. W. (**2024**). Global incidence and mortality of severe fungal disease. *The Lancet Infectious Diseases*, *24*(7), e428–e438.

Deusenbery, C., Wang, Y., & Shukla, A. (**2021**). Recent Innovations in Bacterial Infection Detection and Treatment. *ACS Infectious Diseases*, *7*(4), 695–720.

Dong, J., Wang, N.-N., Yao, Z.-J., Zhang, L., Cheng, Y., Ouyang, D., Lu, A.-P., & Cao, D.-S. (**2018**). ADMETlab: a platform for systematic ADMET evaluation based on a comprehensively collected ADMET database. *Journal of Cheminformatics*, *10*, 1–11.

Eckels, E. C., Chaudhuri, D., Chakraborty, S., Echelman, D. J., & Haldar, S. (**2021**). DsbA is a redox-switchable mechanical chaperone. *Chemical Science*, *12*(33), 11109–11120.

Fernández, C. G. (**2004**). Benzoin, a resin produced by Styrax trees in North Sumatra Province, Indonesia. *Forest Products, Livelihoods and Conservation: Case Studies of Non-Timber Forest Product Systems*, *1*, 148.

Fu, L., Shi, S., Yi, J., Wang, N., He, Y., Wu, Z., Peng, J., Deng, Y., Wang, W., Wu, C., Lyu, A., Zeng, X., Zhao, W., Hou, T., & Cao, D. (**2024**). ADMETlab 3.0: an updated comprehensive online ADMET prediction platform enhanced with broader coverage, improved performance, API functionality and decision support. *Nucleic Acids Research*, *52*(W1), W422–W431.

Garrido, A., Lepailleur, A., Mignani, S. M., Dallemagne, P., & Rochais, C. (**2020**). hERG toxicity assessment: Useful guidelines for drug design. *European Journal of Medicinal Chemistry*, *195*, 112290.

Gnat, S., Łagowski, D., Nowakiewicz, A., & Dyląg, M. (**2021**). A global view on fungal infections in humans and animals: opportunistic infections and microsporidioses. *Journal of Applied Microbiology*, *131*(5), 2095–2113.

Halili, M. A., Bachu, P., Lindahl, F., Bechara, C., Mohanty, B., Reid, R. C., Scanlon, M. J., Robinson, C. V., Fairlie, D. P., & Martin, J. L. (**2015**). Small molecule inhibitors of disulfide bond formation by the bacterial DsbA-DsbB dual enzyme system. *ACS Chemical Biology*, *10*(4), 957–964.

Hsueh, K., Teherani, A., & Guzman-Cottrill, J. A. (**2024**). The Leaders in Epidemiology, Antimicrobial Stewardship, and Public Health (LEAP) Fellowship, a Novel Training Program in Public Health for Infectious Diseases Physicians. *Clinical Infectious Diseases*, *78*(6), 1536–1541.

Inaba, K., & Ito, K. (**2008**). Structure and mechanisms of the DsbB–DsbA disulfide bond generation machine. *Biochimica et Biophysica Acta (BBA) - Molecular Cell Research*, *1783*(4), 520–529.

Iorungwa, M. S., & Wuana, R. A. (**2019**). *Original Research article Synthesis , Characterization , Kinetics , Thermodynamic and Antimicrobial Studies of Fe (III), Cu (II), Zn (II), N , N ' -Bis (2- hydroxy-1 , 2-diphenylethanone) ethylenediamine Complexes*. *May*.

Jesmin, M., Ali, M. M., Salahuddin, M. S., Habib, M. R., & Khanam, J. A. (**2008**). Antimicrobial activity of some schiff bases derived from benzoin, salicylaldehyde, aminophenol and 2, 4 dinitrophenyl hydrazine. *Mycobiology*, *36*(1), 70–73.

Jorgensen, J. H., & Turnidge, J. D. (**2015**). Susceptibility test methods: dilution and disk diffusion methods. *Manual of Clinical Microbiology*, 1253–1273.

Keenan, K., Silva Corrêa, J., Sringernyuang, L., Nayiga, S., & Chandler, C. I. R. (**2025**). The social burden of antimicrobial resistance: what is it, how can we measure it, and why does it matter? *JAC-Antimicrobial Resistance*, *7*(2), 1–10.

Liu, Y., & Cao, Y. (**2024**). Protein–Ligand Blind Docking Using CB-Dock2. *Methods in Molecular Biology*, *2714*, 113–125.

MacKinnon, M. C., McEwen, S. A., Pearl, D. L., Lyytikäinen, O., Jacobsson, G., Collignon, P., Gregson, D. B., Valiquette, L., & Laupland, K. B. (2021). Increasing incidence and antimicrobial resistance in Escherichia coli bloodstream infections: a multinational population-based cohort study. *Antimicrobial Resistance and Infection Control*, *10*(1), 1–10.

Mardani, M. (**2024**). Change in Global Incidence and Mortality of Invasive Fungal Infection. In *Archives of Clinical Infectious Diseases* (Vol. 19, Issue 2).

McQuade, E. T. R., Liu, J., Mahfuz, M., Havt, A., Varghese, T., Shrestha, J., Kabir, F., Yori, P. P., Samie, A., & Saidi, Q. (**2025**). Epidemiology of Shigella species and serotypes in children: a retrospective substudy of the MAL-ED observational birth cohort study. *The Lancet Microbe*.

Miles, S. L., Holt, K. E., & Mostowy, S. (**2024**). Recent advances in modelling Shigella infection. In *Trends in Microbiology* (Vol. 32, Issue 9, pp. 917–924.

Muhammed, M. T., & Aki-Yalcin, E. (**2022**). Molecular Docking: Principles, Advances, and Its Applications in Drug Discovery. *Letters in Drug Design & Discovery*, *21*(3), 480–495.

Naghavi, M., Vollset, S. E., Ikuta, K. S., Swetschinski, L. R., Gray, A. P., Wool, E. E., Robles Aguilar, G., Mestrovic, T., Smith, G., Han, C., Hsu, R. L., Chalek, J., Araki, D. T., Chung, E., Raggi, C., Gershberg Hayoon, A., Davis Weaver, N., Lindstedt, P. A., Smith, A. E., … Murray, C. J. L. (**2024**). Global burden of bacterial antimicrobial resistance 1990-2021: a systematic analysis with forecasts to 2050. *Lancet (London, England)*, *404*(10459), 1199–1226.

Nassar, R., Dignon, G. L., Razban, R. M., & Dill, K. A. (**2021**). The Protein Folding Problem: The Role of Theory. In *Journal of Molecular Biology* Vol. 433, Issue 20, p. 167126.

Okeke, I. N., de Kraker, M. E. A., Van Boeckel, T. P., Kumar, C. K., Schmitt, H., Gales, A. C., Bertagnolio, S., Sharland, M., & Laxminarayan, R. (**2024**). The scope of the antimicrobial resistance challenge. *The Lancet*, *403*(10442), 2426–2438.

Patel, J. B., Tenover, F. C., Turnidge, J. D., & Jorgensen, J. H. (**2011**). Susceptibility test methods: dilution and disk diffusion methods. *Manual of Clinical Microbiology*, 1122–1143.

Paul, J. (**2024**). Introduction to infectious diseases. In *Disease Causing Microbes* (pp. 1–63).

Pieniążek, J. M., Padkowska, A., Dobosz, M., Arciszewska, K., Buczkowski, J., Miazga, M., Paprocki, M., & Mataczyńska, A. (**2024**). Overview Of The Main Bacterial Infections In Humans. *Quality in Sport*, *23*, 54786.

Rather, M. A., Gupta, K., & Mandal, M. (**2021**). Microbial biofilm: formation, architecture, antibiotic resistance, and control strategies. *Brazilian Journal of Microbiology*, *52*(4), 1701–1718.

Rathore, A., Sharma, S., & Sharma, M. (**2025**). Challenges in Infectious Disease Management. In *Sustainable Nanomaterials for Treatment and Diagnosis of Infectious Diseases* (pp. 51–79.

Riedel, J. (**2013**). Distribution - in vitro tests - protein binding. In *Drug Discovery and Evaluation: Safety and Pharmacokinetic Assays, Second Edition*.

Salam, M. A., Al-Amin, M. Y., Salam, M. T., Pawar, J. S., Akhter, N., Rabaan, A. A., & Alqumber, M. A. A. (**2023**). Antimicrobial Resistance: A Growing Serious Threat for Global Public Health. *Healthcare (Switzerland)*, *11*(13).

Salleh, M. Z., Zuraina, N. M. N. N., Deris, Z. Z., & Mohamed, Z. (**2025**). Current trends in the epidemiology of multidrug-resistant and beta-lactamase-producing Pseudomonas aeruginosa in Asia and Africa: a systematic review and meta-analysis. *PeerJ*, *13*, e18986.

Santos-Martin, C., Wang, G., Subedi, P., Hor, L., Totsika, M., Paxman, J. J., & Heras, B. (**2021**). Structural bioinformatic analysis of DsbA proteins and their pathogenicity associated substrates. In *Computational and Structural Biotechnology Journal* (Vol. 19, pp. 4725–4737).

Santoso, P., Sung, M., Hartantri, Y., Andriyoko, B., Sugianli, A. K., Alisjahbana, B., Tjiam, J. S. L., Debora, J., Kusumawati, D., & Soeroto, A. Y. (**2022**). MDR pathogens organisms as risk factor of mortality in secondary pulmonary bacterial infections among COVID-19 patients: observational studies in two referral hospitals in West Java, Indonesia. *International Journal of General Medicine*, 4741–4751.

Sarsamkar, S. K., & Gramopadhye, N. S. (**2021**). Characterization and Antimicrobial Activity of New Cobalt-Nickel-Copper (Ii) Complexes with Benzoin and 3-Amino Benzoic Acid. *SSRN Electronic Journal*, *Ii*.

Saviour Iorungwa, M., Wuana, R. A., & Dafa, S. T. (**2019**). *Chemical Methodologies Synthesis, Characterization, Kinetics, Thermodynamic and Antimicrobial Studies of Fe(III), Cu(II), Zn(II), N,N'-Bis(2-hydroxy-1,2-diphenylethanone)ethylenediamine Complexes*. *3*, 408–424.

Scott, T. A., Baker, K. S., Trotter, C., Jenkins, C., Mostowy, S., Hawkey, J., Schmidt, H., Holt, K. E., Thomson, N. R., & Baker, S. (**2024**). Shigella sonnei: epidemiology, evolution, pathogenesis, resistance and host interactions. *Nature Reviews. Microbiology*, *23*(5), 303–317.

Shouldice, S. R., Heras, B., Walden, P. M., Totsika, M., Schembri, M. A., & Martin, J. L. (**2011**). Structure and function of DsbA, a key bacterial oxidative folding catalyst. *Antioxidants & Redox Signaling*, *14*(9), 1729–1760.

Steward, C. D., Rasheed, J. K., Hubert, S. K., Biddle, J. W., Raney, P. M., Anderson, G. J., Williams, P. P., Brittain, K. L., Oliver, A., & McGowan Jr, J. E. (**2001**). Characterization of clinical isolates of Klebsiella pneumoniae from 19 laboratories using the National Committee for Clinical Laboratory Standards extended-spectrum β-lactamase detection methods. *Journal of Clinical Microbiology*, *39*(8), 2864–2872.

Süssmuth, R. D., Kulike-Koczula, M., Gao, P., & Kosol, S. (**2025**). Fighting Antimicrobial Resistance: Innovative Drugs in Antibacterial Research. *Angewandte Chemie - International Edition*, *64*(10), e202414325.

Thambugala, K. M., Daranagama, D. A., Tennakoon, D. S., Jayatunga, D. P. W., Hongsanan, S., & Xie, N. (**2024**). Humans vs. Fungi: An Overview of Fungal Pathogens against Humans. *Pathogens*, *13*(5), 426.

Tolani, P., Gupta, S., Yadav, K., Aggarwal, S., & Yadav, A. K. (**2021**). Big data, integrative omics and network biology. In *Advances in Protein Chemistry and Structural Biology* (Vol. 127, pp. 127–160.

Trott, O., & Olson, A. J. (**2010**). AutoDock Vina: Improving the speed and accuracy of docking with a new scoring function, efficient optimization, and multithreading. *Journal of Computational Chemistry*, *31*(2), 455–461.

WHO. (2024). WHO bacterial priority pathogens list, **2024**. In *Bacterial pathogens of public health importance to guide research, development and strategies to prevent and control antimicrobial resistance*.

Wiegand, I., Hilpert, K., & Hancock, R. E. W. (**2008**). Agar and broth dilution methods to determine the minimal inhibitory concentration (MIC) of antimicrobial substances. *Nature Protocols*, *3*(2), 163–175.

Yaylı, N., Kahriman, N., Kılıç, G., Serdaroğlu, V., Aliyazıcıoğlu, R., Sellitepe, H. E., Karaoğlu, Ş. A., & Yılmaz, G. T. (**2022**). Molecular docking, synthesis and biological evaluation (enzyme inhibition, antimicrobial and antioxidant) of methoxy benzoin/benzil/stilbenoid derivatives. *Organic Communications*, *15*(2), 129–147.

Yaylı, N., Kılıç, G., Kahriman, N., Kanbolat, Ş., Bozdeveci, A., Alpay Karaoğlu, Ş., Aliyazıcıoğlu, R., Erdinç Sellitepe, H., Selin Doğan, İ., Aydın, A., & Tatar, G. (2021). Synthesis, biological evaluation (antioxidant, antimicrobial, enzyme inhibition, and cytotoxic) and molecular docking study of hydroxy methoxy benzoin/benzil analogous. *Bioorganic Chemistry*, *115*(May).

Zaware, N., Rasal, N., Lambate, V., & Jagtap, S. (**2025**). Biological evaluation of newly synthesized α-benzil monoxime thiocarbohydrazide derivatives as an antimicrobial and anticancer agent: In vitro screening and ADMET predictions. *Bioorganic & Medicinal Chemistry Letters*, *118*, 130079.

ANNEX –I: NMR DATA

Compound 20: ^{1}H- NMR

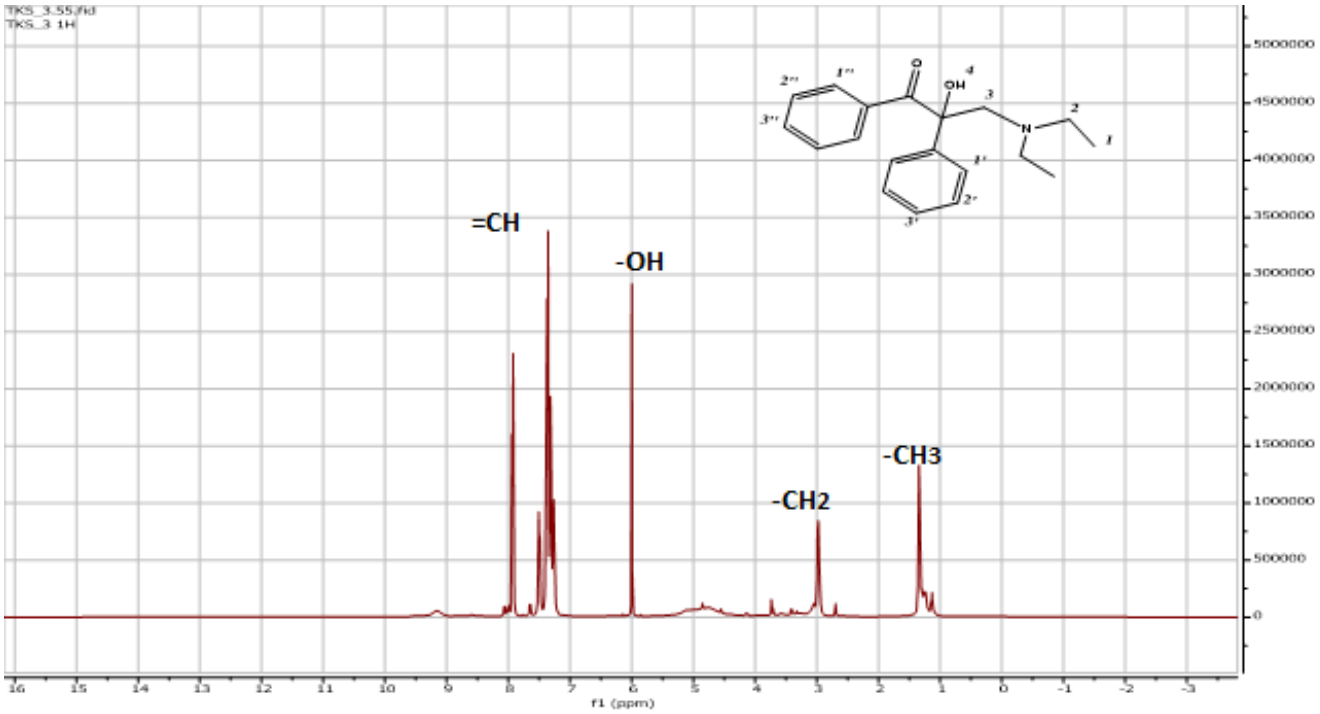

Compound 20: ^{13}C- NMR

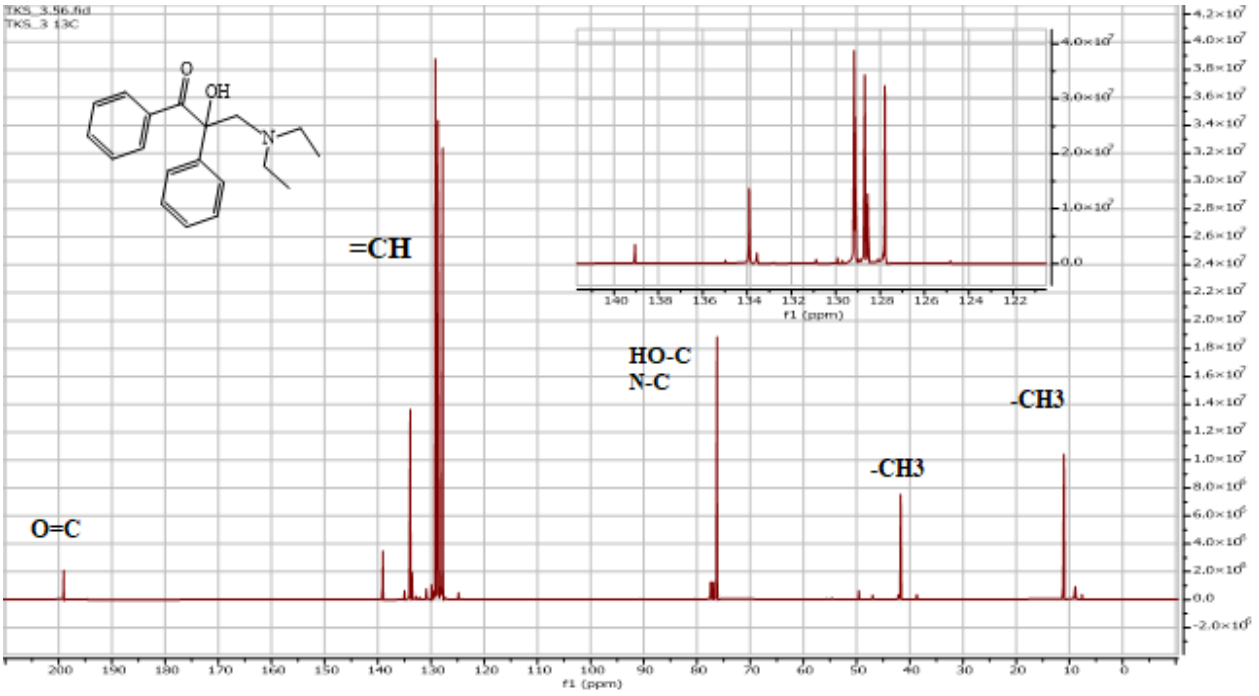

Compound 21: ^{1}H- NMR

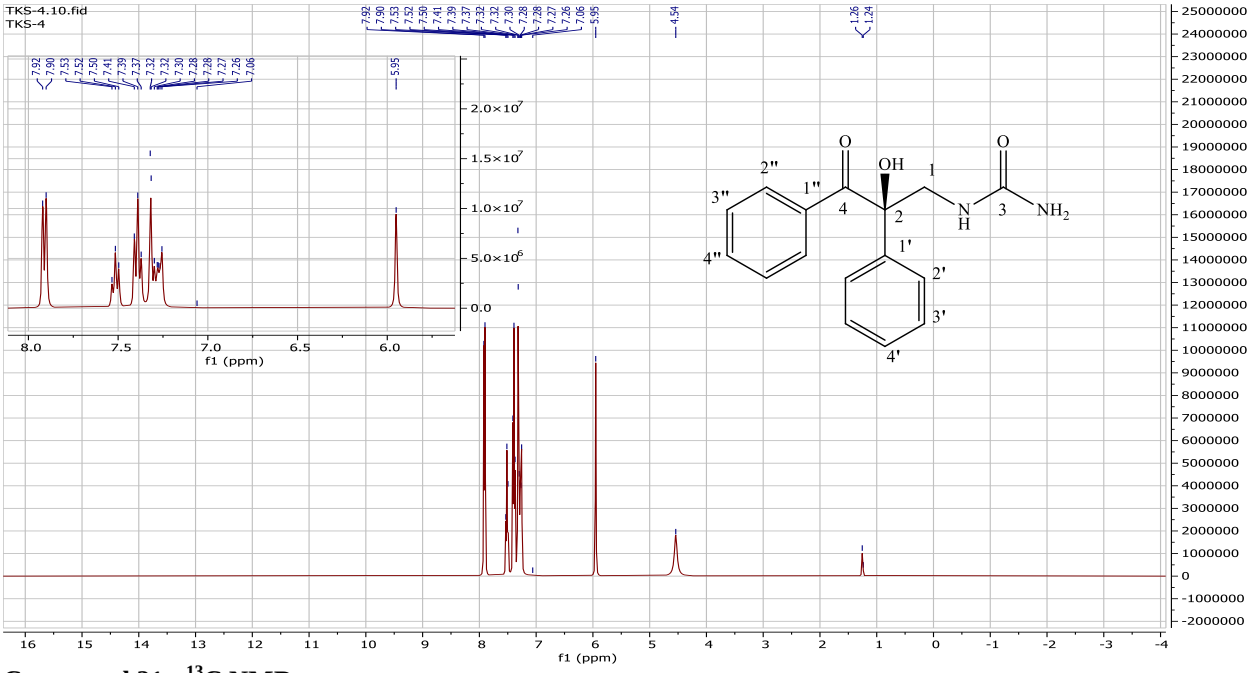

Compound 21: ^{13}C NMR

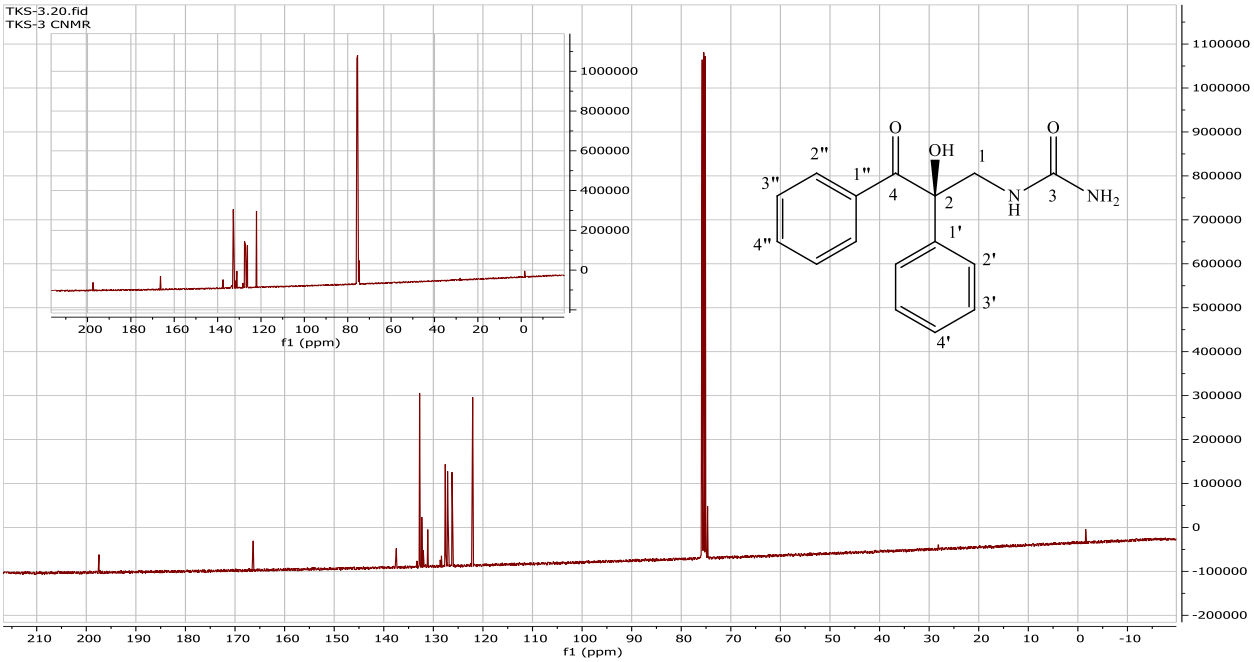

Compound 22: ^{1}H - NMR

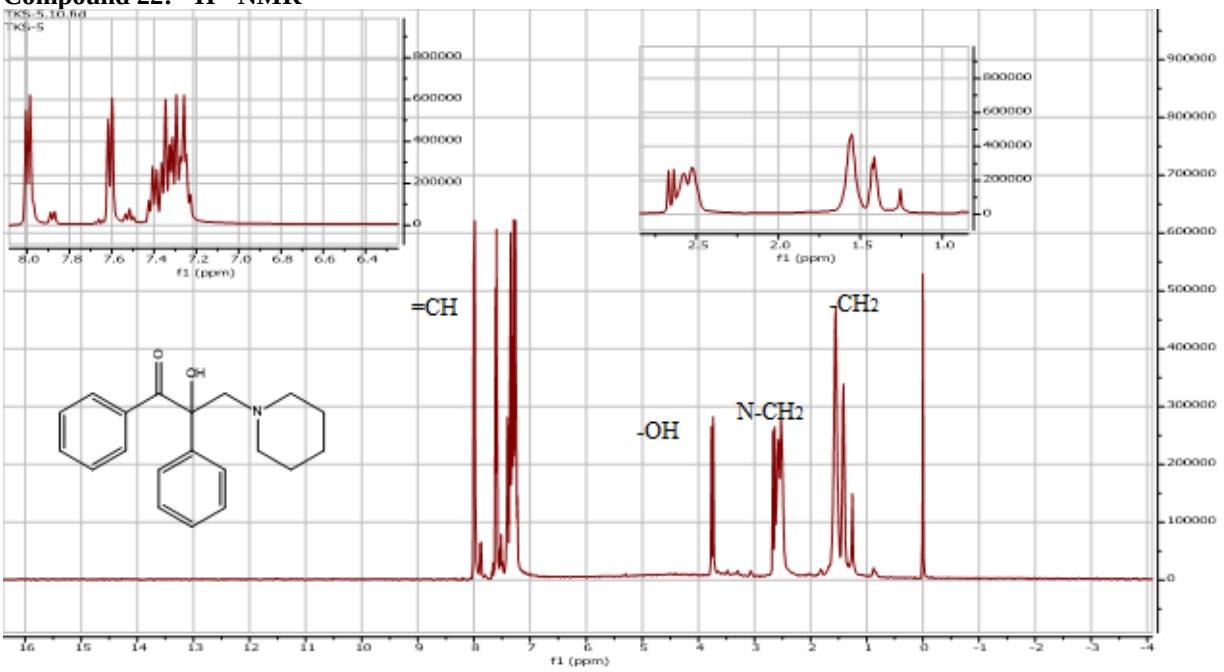

Compound 22: ^{13}C - NMR

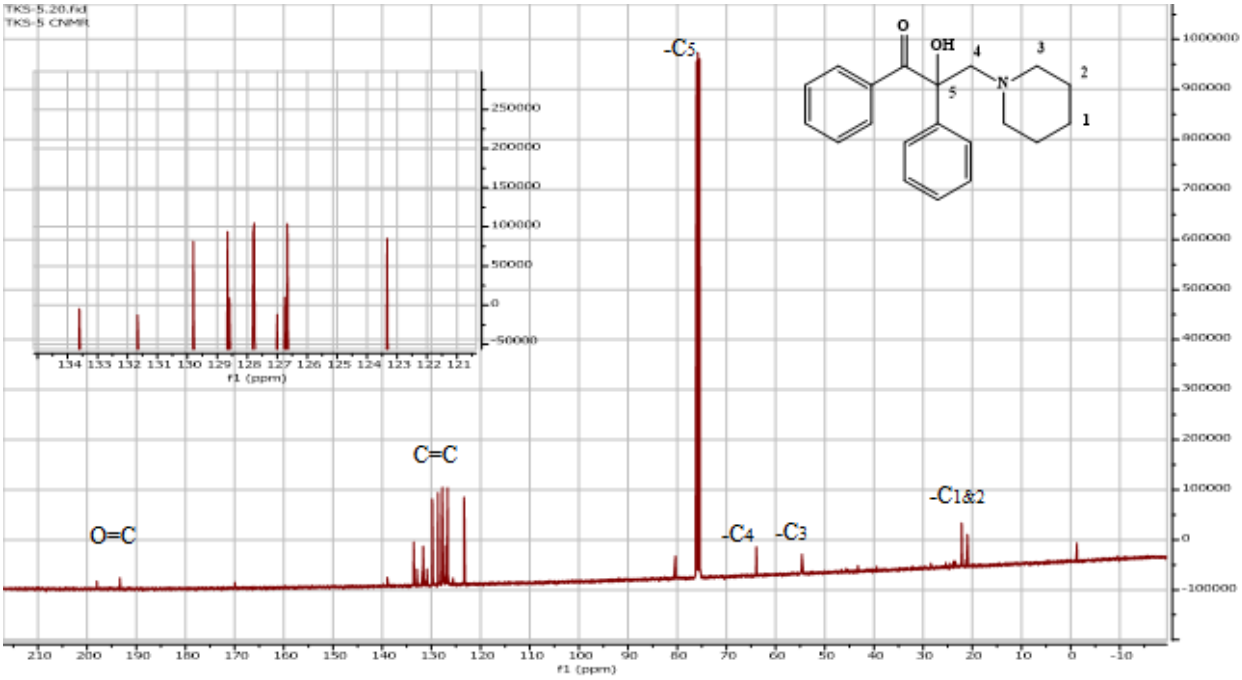

ANNEX-II: TLC Chromatography of the synthesized compounds

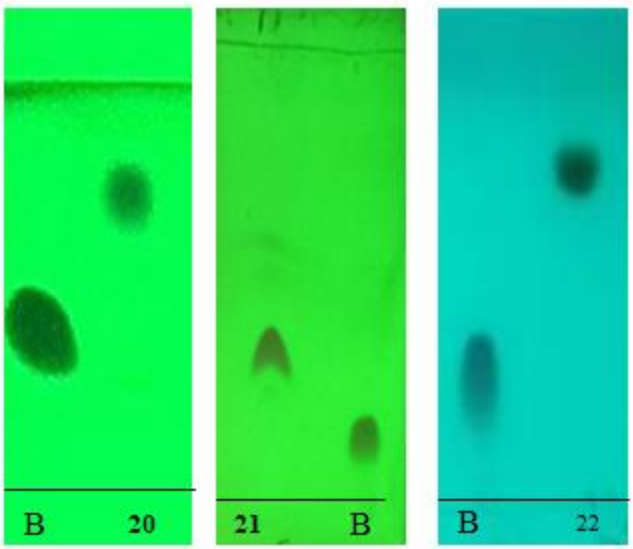

Figure 5: Normal Phase TLC chromatograms of compound 20, 21 & 22 viewed under UV 254 using solvent system HE/CF (2:1)

ANNEX-III: Binding interactions of the synthesized compounds 20, 21 and 22 with E. coli DsbA

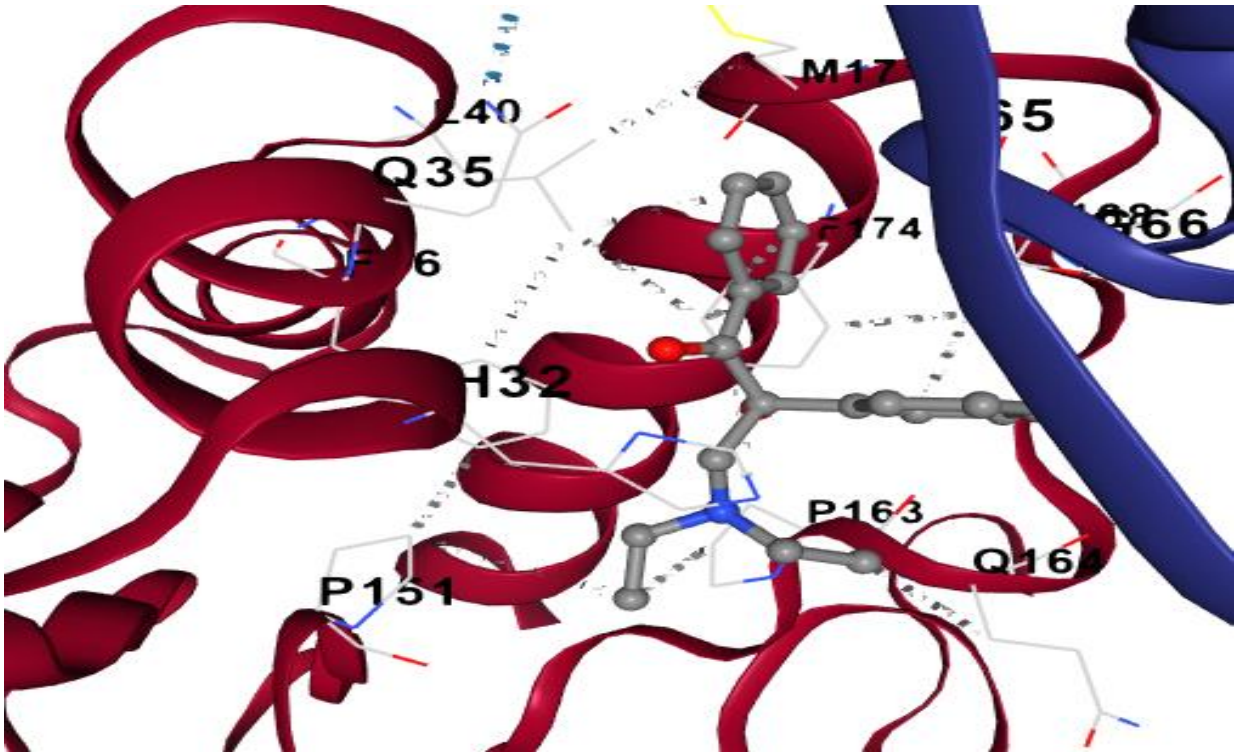

Figure 6**:** Compound **20** complexes with E. coli DsbA in CB-Docing (PDB ID = 8DN0)

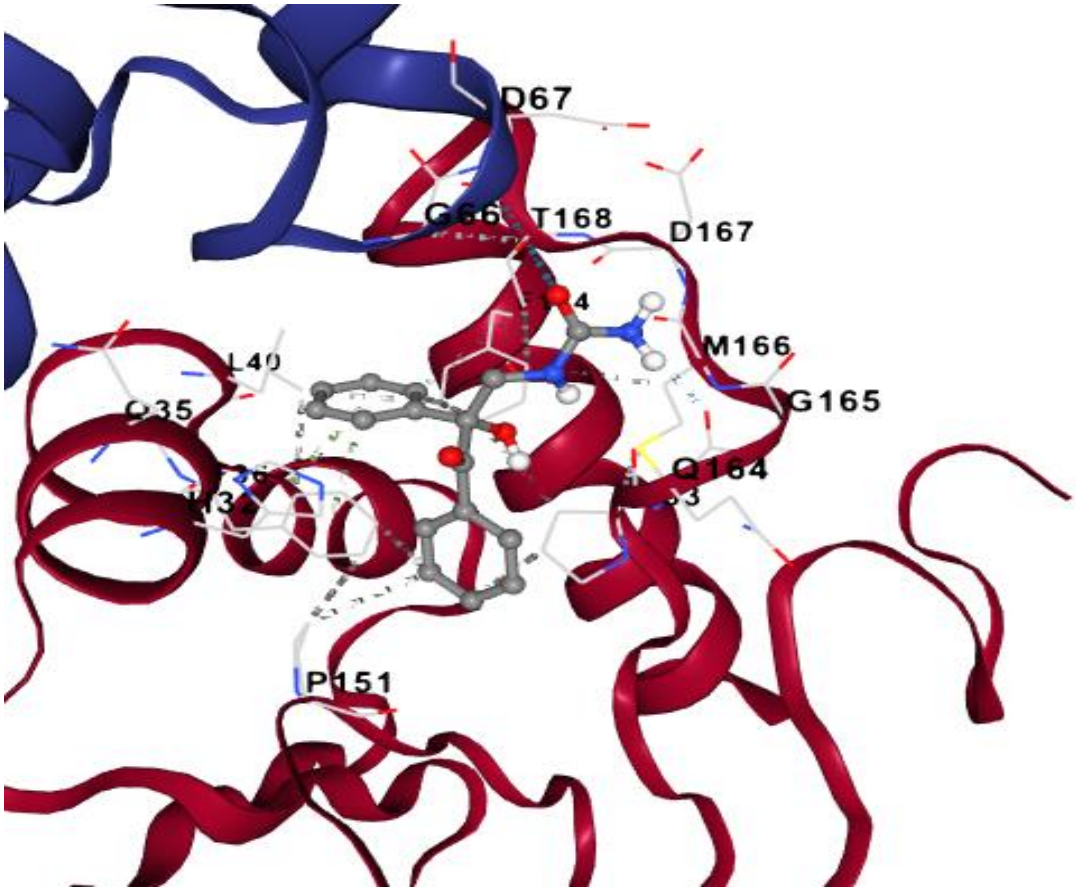

Figure 7: Compound **21** complexes with E. coli DsbA in CB-Docing (PDB ID = 8DN0)

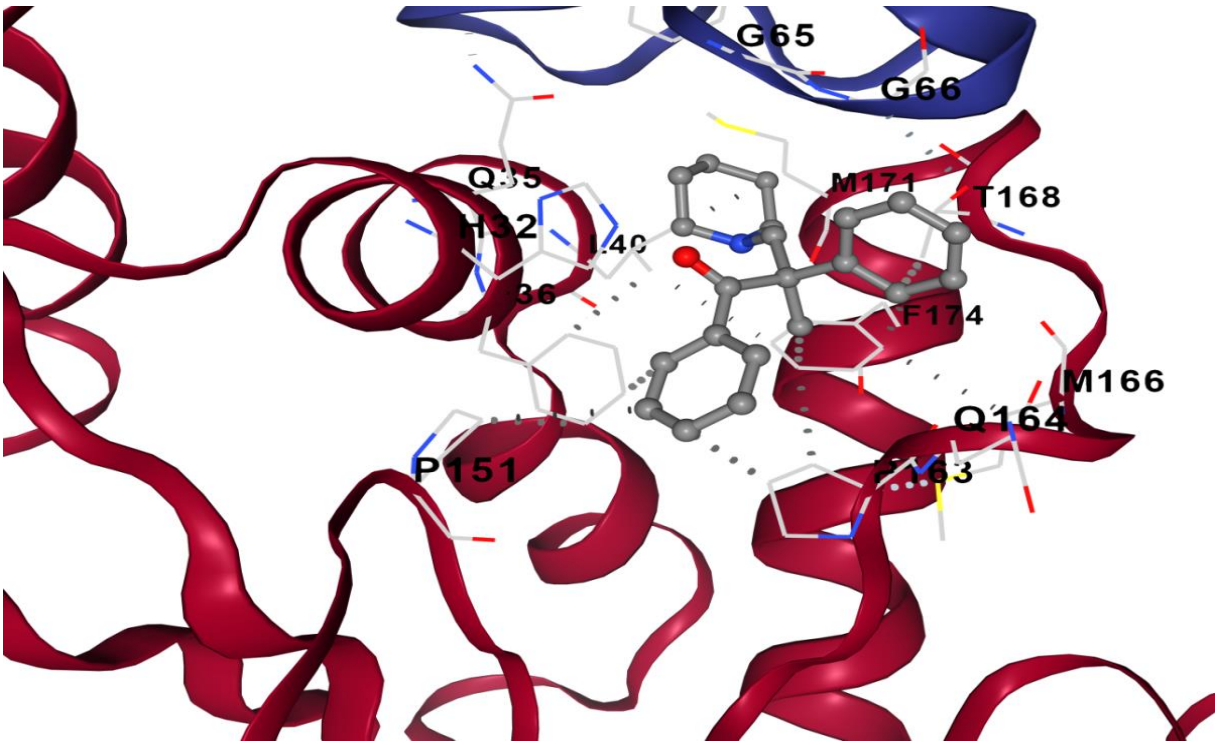

Figure 8: Compound **22** complexes with E. coli DsbA in CB-Docking (PDB ID = 8DN0)

Draft manuscript from the thesis

Synthesis, anti-bacterial, and *in silico* studies of 2-hydroxy-1, 2-diphenylethanone Derivatives

Temesgen Kusse[1], Daniel Bisrat[2], Kaleab Asres[2] Prof. Avijit Mazumder[3]

1. Department of Pharmacy, pharmaceutical Unite, College of Medicine and Health science, Arba Minch University, Ethiopia.
2. Department of Pharmaceutical Chemistry and Pharmacognosy, School of Pharmacy, Addis Ababa University, Ethiopia.
3. The Central Drugs Laboratory in Kolkata, the Department of Technology at Jadavpur University, India.

Abstract

Infectious diseases place a significant impact on the healthcare system. It causes 7.7 million fatalities each year, with a disproportionately high burden in sub-Saharan Africa. Drug resistant pathogens attributed to 4.95 million are and 1.27 million are brought on by illnesses of bacteria that are resistant to the current medications. Therefore, there is an urgent need for new, safe, and effective compounds to combat antimicrobial resistance (AMR). In this context, 2-hydroxy-1,2-diphenylethanone has emerged as a valuable precursor in medicinal chemistry, attracting significant interest for the development of novel bioactive molecules. The aim of this study was to synthesize new compounds derived from 2-hydroxy-1,2-diphenylethanone using the Mannich reaction and to evaluate their antibacterial and antifungal activities against 26 bacterial strains and 4 fungal strains. Three compounds were successfully synthesized and their structures were confirmed as 2-hydroxy-1,2-diphenyl-3-(piperidin-1-yl)propan-1-one (**20**), 1-(2-hydroxy-3-oxo-2,3-diphenylpropyl)urea **(21),** and 3-(diethylamino)-2-hydroxy-1,2-diphenylpropan-1-one **(22)** using ^{1}H and ^{13}C-NMR spectroscopy. All the synthesized compounds exhibited broad-spectrum antibacterial activity. Among them, compound **21** demonstrated the highest activity, with a

minimum inhibitory concentration (MIC) of 10 µg/mL against *Shigella sonnei* 1, *Shigella boydii* D13629, and *Pseudomonas aeruginosa* MDR1.

Furthermore, synthesized compounds exhibited Antifungal activity. Among them, compound **22** demonstrated the highest activity, with a minimum inhibitory concentration (MIC) of 200 µg/mL against *Candida albicans* ATCC 10231, *Aspergillus niger* ATCC 6275, *Penicillium funiculosum* NCTC 287, and *Penicillium notatum* ATCC 11625.

Molecular docking studies were performed to predict the potential mechanism of action of the synthesized compounds. The results showed that the compounds interact favorably with conserved residues in the binding site of *E. coli* DsbA (PDB ID: 8DN0) through hydrogen bonding and hydrophobic interactions, with docking scores of –7.5 kcal/mol **21**, –7.1 kcal/mol **22**, and –6.5kcal/mol **20**. The current work suggests verify the molecular docking results experimentally, biological activities for the three 2-hydroxy-1, 2-diphenylethanone derivatives, such as antiviral, anticancer, anti-inflammatory, and antioxidant properties and evaluate the safety profile of the produced chemicals, conduct thorough toxicity tests.

Keywords: 2-hydroxy-1, 2-diphenylethanone, Antimicrobial activity, *in-silico* studies, Disulfide bond oxidoreductase (DsbA), Mannich reaction

1. Introduction

Infectious ailments are illnesses caused by dangerous microbes such as bacteria, viruses, fungi, or parasites that attack the body (Berkelman et al., 1994). It places a significant strain on the healthcare system. In 2022, infectious diseases affected around 900 million individuals, which result 7.7 million fatalities each year. (Okeke et al., 2024; Rathore et al., 2025). With a high burden in sub-Saharan Africa (Paul, 2024) ranging from asymptomatic to potentially fatal, are brought on by bacteria (Pieniążek et al., 2024).

Benzoin (2-hydroxy-1, 2-diphenylethanone) (**1**) is organic molecule with ketone, alcohol, and aromatic phenyl functional groups. It possesses several pharmacological properties, including antimalarial, antifungal, antioxidant, anticancer, and antibacterial properties (Sarsamkar & Gramopadhye, 2021; Yaylı et al., 2022). As a natural product benzoin it's produced by *Styrax* trees' as resin and utilized for flavoring ingredient, incense, and perfume. In many parts of the world, it has been grown for thousands of years for use as to treat wounds, skin conditions, neurological issues, anxiety, and muscle soreness (Atia Sharif et al., 2016; Fernández, 2004).

Different compounds contains benzoin was synthesized by Schiff base like N-(2-hydroxy benzylidine)-2'-hydroxy imine (**2**) and sulfamethazine derivatives (**3**) hold considerable promise for developing new antimicrobial agents (Buran, 2025). This made an interest in benzoin's and their derivatives in the medicinal chemistry for the synthesis of several essential organic functional groups and high-profile biologically active natural compounds (Babu Kothapalli et al., 2025).

A growing threat to global health, antimicrobial resistance (AMR) is being measured increasing in terms of its impact on human health and the economy (Keenan et al., 2025). In addition to

issues with drug interactions and antimicrobial resistance, there is a lack of recently approved antibiotics on the market. The Research & Development pipeline for novel medicines and new resistance patterns are also reflected (WHO, 2024).

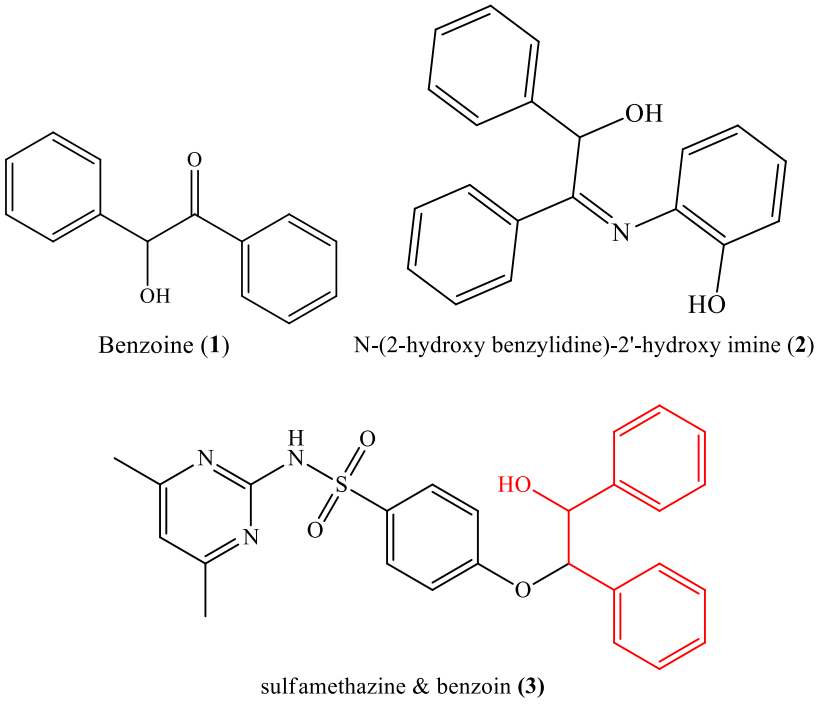

Benzoine (**1**) N-(2-hydroxy benzylidine)-2'-hydroxy imine (**2**)

sulfamethazine & benzoin **(3)**

Schem 1: Different compounds contains benzoin

2. Methods

2.1. Chemical Material and Apparatus

The chemicals used are Methanol (99.6%), n-hexane (99.8%), Chloroform 99.8%), Diethyl ether (99.9%), ethanol (99.6%), bought from LOBA chemie Pvt.Ltd. and all are HPLC graded. Sulphuric acide, hydrochloric acide, Benzoin 2,4-dinitrophenyl Hydrazine, Urea, Formaldehyde, Peperidine, N,N-Diethyl amine Benzidine,. DMSO, (PBH), obtained from Addis Ababa University school of Pharmacy Pharmaceutical and Pharmacognosy lab. TLC plates (60-120 mesh Per-coated plastic Sheet POLYGRAM SIL G/UV_{254} with layer of 0.2mm thick Germany),

for reaction monitoring and analytical, filter paper Watman No-1 (90mm), Water bath, Micro-pipette (10-200μl), Rota evaporator (Hiedolph Laborota 4001 efficient Germany), Vacuum pump V-700 (BHUCHI Labortechin AG Switzerland) for removal of the solvent, ARXE-Heat, reaction flask, and Magnetic stirrer, for the reaction, UV-Visible Spectrophotometry (UV-CAMAG), was used to visualize the TLC plates and electronic balance (SICENTHECH SA) for weighing amount of the chemicals. NMR spectra were recorded using 400MHz for ^{1}H and 100MHz for ^{13}C NMR on a Bruker Adivance DMX400 FT-NMR Spectrometry (Bruker Billerica Idaho, USA), tetiramethyl silane (TMS) for the internal standard and detureted chloroform ($CDCl_3$) as a solvent for the NMR Spectroscopy. Incubator (Model 100-800 memmert), autoclave, biosafety cabinet (model) and inoculating loops are used for anti-microbial assay.

2.2. Synthesis

General synthesis of 2-hydroxy-1, 2-diphenylethanone derivatives was achieved through benzoin condensation reactions typically involves the condensation of benzoin with amines to form Schiff base ligands (Iorungwa & Wuana, 2019) and followed by Mannich reaction involves the formation of β-amino ketones (Blicke, 1942).

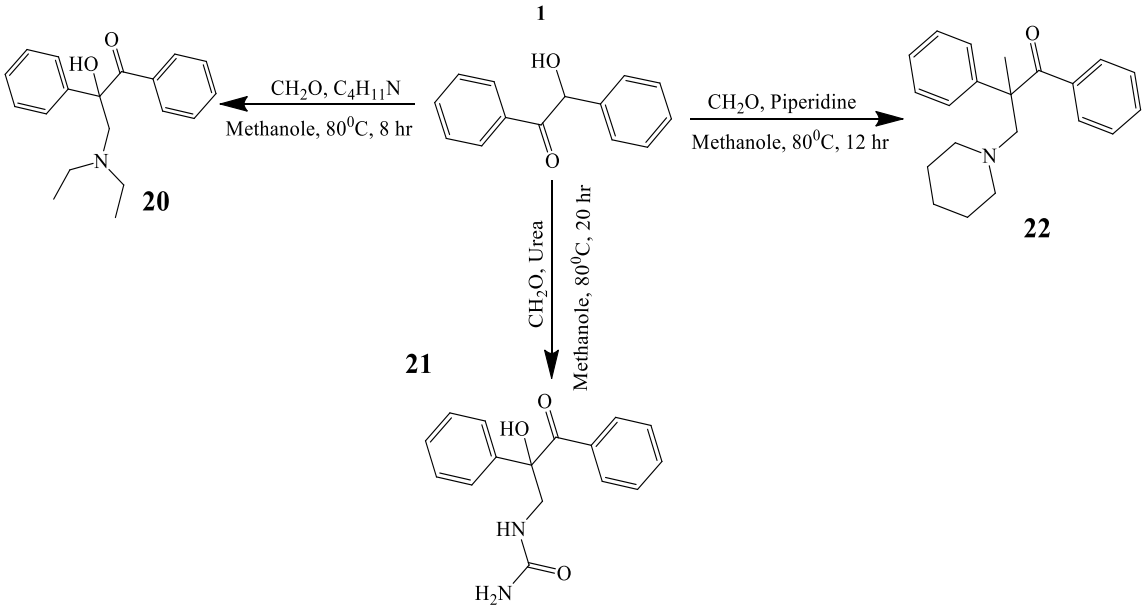

Schem 2: General synthesis of 2-hydroxy-1, 2-diphenylethanone derivatives

3.2.1. *Synthesis of 3-(diethyl amino)-2-hydroxy-1, 2 diphenylpropan-1-one) (20*)

3-(diethyl amino)-2-hydroxy-1, 2-diphenylpropan-1-one is synthesized by initially 30 mL of methanol was added in to a 100 mL of reaction flask, then 0.83g (4.00 *m*mol) of Benzoin was added to the reaction flask containing methanol and stirred at $50^{O}C$ by magnetic terrier until it completely dissolve and added four drops of concentrated sulphuric acide as catalyst. In another beaker 0.36g (1.334mmol) of diethyl amino was dissolved in 20 mL methanol and the solution was added stepwise to the reaction flask containing Benzoine. Then it was stirred at temperature of $80^{o}C$ at stirring rate of 500 revolutions per minute (rpm) and the reaction completion was monitoring with TLC every 60 minute for 8- hour. Then, the product was poured in round bottom flask and the solvent was removed by rotavouper at temperature of $80^{o}C$ and rotation of 100 rpm until it dried. Then after, the dried product was collected and run a flash column

chromatogram for further purification with an increasing gradient of hexane in ethylacetet as the eluting solvent.

3.2.2. Synthesis of 1-(2-hydroxy-3-oxo-2, 3-diphenylpropyl) urea (21)

It was synthesized by the process of Mannich reaction. Initially 20 mL of methanol was added in to a 100 mL of reaction flask, then 0.85ml of 37% solution of formaldehyde and added four drops of concentrated Sulphuric acide as catalyst. Then 0.6g of urea was added to the reaction flask. In another beaker 2.0 g/4.00 mmol of Benzoin was dissolved in 30ml of methanol & added to the reaction flask and stirred at 50 ^{O}C and the reaction completion was monitoring with TLC every 60 minute for 20- hour. Then, the product was poured in round bottom flask, and the solvent was removed by rotavouper at temperature of 50^{0}C and rotation of 100 revolutions per minute (rpm) until it dried. Then after, the dried product was collected and run flash column chromatogram for further purification.

3.2.3. Synthesized of 2-hydroxy-1, 2-diphenyl-3-(piperidin-1-yl) propan-1-one (22)

It is synthesized by adding 20 ml methanol into a 100 mL of reaction flask, then 0.68ml of 37% solution of formaldehyde and added four drops of concentrated Sulphuric acide as catalyst. Then 0.85g (2ml) of Peperidine was added to the reaction flask. In another beaker 2.0 g/4.00 mmol of Benzoin was dissolved in 30ml of methanol & added to the reaction flask and stirred at 80 OC and the reaction completion was monitoring with TLC every 60 minute for 12- hour. Then, the product was poured in round bottom flask, and the solvent was removed by rotavouper at temperature of 80oC and rotation of 100 revolutions per minute (rpm) until it dried. Then after, the dried product was collected and run flash column chromatogram for further purification with an increasing gradient of hexane in ethylacetet as the eluting solvent.

3.3. Structural confirmation of the synthesized compounds

The structures of compounds **20, 21** and **22** were identified by analyzing their ^{1}H and ^{13}C-NMR spectra data. The chemical shifts are denoted in ppm and coupling constants (J) are expressed in Hz. Signal multiplicities are indicated as follows: *s* = singlet; *d* = doublet; *t* = triplet; *ddd* = doublet of doublet of doublets; and *m* = multiplet.

3.4. In vitro antibacterial and antifungal activity assay.

3.4.1. Disk diffusion method

The disc diffusion method was used to screen the in vitro antibacterial assay by evaluating the zones of inhibition generated by the test samples. It is a time-consuming method that requires antimicrobial disk diffusion testing and interpretation (Daliri Shamsabadi, 2024; Jorgensen & Turnidge, 2015)

By making a stock solution of 1 mg/mL of the benzoin derivatives in 1% DMSO, the antibacterial and antifungal effects of the chemicals produced were investigated. The antibacterial and antifungal activity test values ranged from 5 to 800µg/mL for antibacterial and from 50 to 2000 µg/mL antifungal. Then the stock solution was diluted in the proper amounts of distilled water. After that, sterile Petri dishes were filled with molten media and incubated for 24 hours at 37 °C to check for contamination in order to create the serial nutritional agar plates. After serial nutrient production, the inoculums were evenly swabbed and left to dry for five minutes. The Petri plates were subsequently incubated for 24 hours at 37 °C, and the diameter of the inhibitory zone was determined in millimeters. The experiment was performed using 1% DMSO as a negative control and ciprofloxacin as a positive control for bacteria. The Zone of inhibition (ZOI) was then compared.

On Saborauds dextrose media, the test samples' antifungal potential was evaluated using an identical methodology against the fungal infections. Millimeters were used to measure the ZOI's diameter in the Petri plates following three days of room temperature incubation. The Griseofulvin was used in this instance as the standard drug.

2.2.1. Broth dilution method

The minimum inhibitory concentration (MIC) of the produced compounds was determined using broth dilution procedure (Steward et al., 2001). The Mueller–Hinton broth and Saborauds dextrose broth were used for bacterial growth and fungal, respectively. The produced compounds were dissolved in 1% DMSO at concentrations of 5, 10, 25, 50, 100, 200, 400, and 800µg/mL for the antibacterial activity test and 50, 100, 200, 400, 800, 1000, 1500, and 2000 µg/mL for the antifungal activity test.

A sterility control, which involves growth control using nutritious broth and DMSO devoid of antibiotics, was also carried out. Each test well and growth control well was cultured for three days at 25 °C for fungi and for twenty-four hours at 37 °C for bacteria. MIC was indicated by the test tubes' lack of turbidity (Wiegand et al., 2008).

3.5. In silico study

3.5.1. Molecular docking

A protein-ligand docking technique called CB-Dock automatically finds the binding sites, determines their size and center, and adjusts the docking box's dimensions based on the query ligands. The hit percentage and accuracy of blind docking can be improved by cavity-focused docking, according to extensive benchmarking. As a result, CB-Dock can speed up the docking

process and increase accuracy by employing our curvature-based cavity detection method to forecast the target proteins' binding locations (Trott & Olson, 2010). CB-Dock workflow comprised six stages: Input and Preprocessing, Cavity Detection, Grid Generation, Docking Simulation with Autodock Vina, Score Ranking & Results Visualization and Output.

3.5.2. Pharmacokinetics and drug-likeness properties

With the aid of the online software tool ADMET lab 3.0, the physicochemical, pharmacokinetic, and toxicity characteristics of the produced compounds were anticipated, as described by J. Dong *et al* 2013 (Dong et al., 2018).

4. RESULT AND DISCUSSION

In this study, three compounds, 3-(diethylamino)-2-hydroxy-1,2-diphenylpropan-1-one (**20**), 1-(2-hydroxy-3-oxo-2,3-diphenylpropyl)urea (**21**), and 2-hydroxy-1,2-diphenyl-3-(piperidin-1-yl)propan-1-one (**22**), were successfully synthesized from 2-hydroxy-1,2-diphenylethanone using a one-pot reaction. The synthesis followed a Mannich-type reaction pathway, leading to the formation of *β*-amino alkylation products. The physical properties of these compounds table 1: below.

Table 12: Physical properties of the synthesized compounds

Compound	**MF**	**MW**	**Colour**	**PS**	**Yield**	***R_f value***
20	$C_{19}H_{23}NO_2$	297.37	White	Crystal	56%	0.7
21	$C_{17}H_{17}NO_3$	283.32	White	Crystal	87%	0.4
22	$C_{20}H_{23}NO_2$	309.40	Yellowish	Powder	64%	0.8

Key: MF=Molecular formula, MW= Molecular weight, PS= Physical state, R_f = Retention factor

3.1. Structural confirmation of 3-(diethylamino)-2-hydroxy-1, 2-diphenylpropan-1-one

Compound **20** was successfully synthesized as a white crystal (2.4mmol. M.wt 297.37) with an R_f value of 0.7 The ^{1}H-NMR spectrum displayed a triplet at δ 1.24 ppm (3H, *J*=6.7 Hz, H-1) and a quartet at δ 2.96 ppm (2H, *J*=6.8 Hz, H-2), consistent with an ethyl group (–CH_2CH_3) moiety. A pair of doublets at δ 3.00 and 3.08 ppm (H-3) suggested diastereotopic methylene protons adjacent to an electronegative group or stereocenter. A singlet at δ 6.00 ppm corresponded to a hydroxyl (OH) proton, indicating the presence of a free phenolic or alcoholic group. Aromatic

proton signals appeared as multiplets and doublets in the region δ 7.40–7.94 ppm, characteristic of substituted aromatic rings..

The ^{13}C-NMR (126 MHz, $CDCl_3$) demonstrates the presences of two methyl groups C-1 (δ=11.01), the presence of methylene carbon C-2&3 ((δ=41.73 & 50.93), also quaternary carbon at (δ=77.44) and aromatic carbons. (See table 2 and annex). Thus, the structure of compound **20** was confirmed by both 1H-NMR and 13C-NMR investigations.

4.2. Structural confirmation of 1-(2-hydroxy-3-oxo-2, 3-diphenylpropyl) urea

Compound **21** was successfully synthesized as a white crystal (2.4mmol. 24%w/w, M.wt 201.26) with an R_f value of 0.4 on TLC using HE/CF (2:1) as the mobile phase. The ^{1}H NMR (500 MHz, CDCl3) of **21** shows that total of ten sets of proton. Among those one methylene protons assigned to H-$_1$(δ=4.45, *d*, *J* =11.04Hz), three amine protons assigned to NH &NH_2 (δ=5.96, *s*,) two methylene protons assigned to H-3(δ=2.96, *d*, *J* =11.9Hz) one hydroxyl proton –OH (δ=6.00, *s*) six set of aromatic protons on two phenyl rings.

The ^{13}C-NMR (400 MHz, $CDCl_3$) demonstrates the presences of one methylene Carbone assigned to C_{-1} (δ=55.23), the presence one of quaternary carbon C_{-2} at (δ=77.23), carbonyl carbon of the amide at (δ=167.32), carbonyl carbon of the ketone at (δ=197.78) and aromatic carbons. Thus, the structure of compound **21** was confirmed by both 1H-NMR and 13C-NMR investigations.

4.3. Structural confirmation of 2-hydroxy-1, 2-diphenyl-3-(piperidin-1-yl) propan-1-one

Compound **22** was synthesized as a yellowish powder (2.4mmol. 24%w/w, M.wt 309) with an R_f value of 0.8 on TLC using HE/CF (2:1) as the mobile phase. The ^{1}H NMR (400 MHz, CDCl3) of

22 shows that total of eleven sets of proton. Among those eight methylene protons assigned to $H_{1\text{-}4}$, one hydroxyl protons, ten aromatic protons on two phenyl rings. The two methylene protons assigned to $H_{1\&2}$(δ = 1.13 - 159, *m*, *J* = 6.7) one hydroxyl proton H-4(δ=3.74, *s*,) The ^{13}C-NMR (101 MHz, $CDCl_3$) demonstrates the presences of four methylene groups C-1 (δ=11.01), the presence of methylene carbon C-2&3 ((δ = 41.73 & 50.93), the also quaternary carbon at (δ=77.44) and aromatic carbons. Thus, the structure of compound **22** was confirmed by both ^{1}H-NMR and ^{13}C-NMR investigations.

4.4. Antimicrobial activity of the synthesized compound

4.4.1. Antibacterial activity

In this research 2-hydroxy-1, 2-diphenylethanone derivatives were synthesized **20, 21** and **22** tested *in vitro* against 26 bacterial strains by both disc diffusion and broth dilution method. Surprisingly, three of them were demonstrates similar antibacterial activity with MICs ranging from 10 µg/mL to 800 µg/mL and Zone of inhibition ranging from 6.0mm to 15.8mm. Among the three synthesized compounds the maximum activity against *Shigella soneii* 1, *Shigella boydii* D13629, and *Pseudomonas aeruginosa MDR1* which is 10µg/mL by **21**

Table 13: Zone of inhibition and minimum inhibitory concentration of synthesized compounds against the tested bacterial strains.

	ZOI in mm (200µg/ml)				**MIC (µg/ml)**		
Bacteria strain	**20**	**21**	**22**	**Ciprofloxacin**	**20**	**21**	**22**
E.coli K99	13.5	12.2	13.5	16.0	25	100	25
E.coli K88	14.8	12.5	14.8	17.0	25	100	25
E.coli 306	14.0	13.0	14.3	17.0	25	100	25
E.coli LT37	14.0	12.5	14.0	16.0	25	100	25
E.coli 872	14.5	12.7	14.5	15.8	25	100	25
E.coli ROW 7/12	15.0	12.0	14.5	16.5	25	100	25
E.coli 3:37C	15.2	11.8	15.2	16.5	25	100	25

E.coli CD/99/1	15.7	12.2	15.7	16.8	25	100	25
Salmonella typhi Ty2	13.2	13.7	11.8	16.0	400	100	800
Salmonella enterica TD 01	14.2	14.0	12.7	19.0	400	100	800
Shigella dysentery 8	13.8	13.7	13.8	20.0	100	100	100
Shigella soneii 1	14.0	15.8	14.0	19.5	50	10	50
Shigella boydii D13629	14.0	15.8	14.0	20.0	50	10	50
Shigella flexneri Type 6	15.8	15.5	15.8	20.5	50	50	50
Staphylococcus aureus MDR10	14.3	14.7	14.3	18.0	100	400	100
Bacillus pumilus 82	9.0	6.0	8.0	18.8	200	400	800
Bacillus subtilis ATCC 6633	10.2	6.0	7.5	18.0	200	400	800
Vibrio cholerae 1313	12.0	13.3	12.0	17.5	100	25	100
Vibrio cholerae 293	12.3	14.7	12.3	18.7	100	25	100
Vibrio cholerae 1315	11.3	14.8	11.3	19.0	100	25	100
Vibrio cholerae 85	11.2	14.0	11.5	18.5	100	25	100
*E.coli HB101**	13.2	14.0	12.2	16.0	200	25	100
*E.coli C600**	13.0	13.8	12.8	16.0	200	25	100
*S.aureus MDR 1**	14.2	14.2	14.3	18.0	100	25	100
*S.aureus MDR 2**	14.3	14.7	14.3	18.0	100	25	100
*Pseudomonas aeruginosa MDR 1**	14.0	14.8	13.0	17.3	200	10	50

Key: *ZOI = Zone of Inhibition, MIC = Minimum Inhibitory Concentration*

4.4.2. Antifungal Activity

Benzoin (2-hydroxy-1, 2-diphenylethanone) derivatives were synthesized **20, 21** and **22** and *in vitro* tested against four strains of fungal species were demonstrated by both disc diffusion and broth dilution method with antibacterial activity of MICs ranging from 200 µg/mL to 1000 µg/mL and Zone of inhibition ranging from 12 mm to 15 mm.

Table 14: Zone inhibition and minimum inhibitory concentration of Synthesized compound against the tested fungal species.

	ZOI (2000 µg/ml)			**MIC (µg/ml)**	**MIC (µg/ml)**		
Fungi	**20**	**21**	**22**	**Griseofulvin**	**20**	**21**	**22**
Candida albicans ATCC 10231	12.0	12.5	15.0	16.0	1000	1000	200
Aspergillus niger ATCC 6275	13.0	14.0	15.0	15.0	400	800	200

Penicillium notatum ATCC 11625	13.5	14.5	15.0	15.0	800	800	200
Penicillium funiculosum NCTC 287	13.0	12.5	15.0	14.0	800	800	200

Key: *ZOI = Zone of Inhibition, MIC = Minimum Inhibitory Concentration*

4.5. *In silico* Studies

4.5.1. Pharmacokinetics and drug-likeness properties

The findings of this study showed that three of compounds exhibited good intestinal absorption, volume of distribution and plasma protein binding which is important for their effectiveness. However, three of them had low blood-brain barrier (BBB) profiles, making them less suitable for meningeal infections as shown in Table 9, ADMETlab 3.0 software prediction.

Three of the compounds are none inhibitors of CYP enzymes. However, **22** are substrates for *p-gp*, indicating it can be effluxed pumped out from the cell. The compounds **21** & **22** demonstrated poor clearance. However, compound **20** & **22** poses a risk of hERG (human ether-ago-go related gene) toxicity, potentially leading to cardiac arrhythmia (Garrido et al., 2020).

We evaluated and contrasted three compounds' drug-likeness using Lipinski's rule of five. Lipinski's rule of five, which states that a molecule must have a molecular weight (MW) of less than 500, a log P (partition coefficient) of less than 5, hydrogen bond donors of less than 5, and hydrogen bond acceptors of less than 10, was met by three of the synthesized compounds. The synthesized compounds are expected to follow Lipinski's

Moreover, we evaluated the synthetic compounds' toxicities, paying attention to cardiotoxicity, mutagenicity, and drug-induced liver damage. Both acute and chronic liver illnesses are known to result from drug-induced liver damage, which is particularly brought on by drugs. Three of the

produced chemicals were anticipated to have negative effects on the liver, according to the data. Compound **21** showed toxicity in the Ames test for mutagenicity. Two compounds **20** and **22** were shown to be inhibitors when we examined their ability to block potassium channels encoded by hERG (human ether-a-go-go-related gene), a major contributing factor to the development of deadly ventricular arrhythmias.

4.5.2. Molecular docking

The synthesized compounds were subjected to molecular docking with the *E.coli* DsbA in complex with N-(2-fluorophenyl)-5-methylisoxazole-3-carboxamide structure, obtained from PDB (ID = 8DN0) (B., 2023) was used in order to evaluate the synthetic chemicals' binding affinity inside active site of the *E.coli* DsbA enzyme.

Compound **21** had the most advantageous docking score of -7.5kcal/mol, according to the molecular docking study results. Compound **22** came in second with a docking score of -7.1kcal/mol beneficial relationships with E. coli DsbA as shown below in the figure 2: to figure 5. The produced compounds demonstrated adequate binding to the *E. coli* DsbA enzyme.

Furthermore, through a number of π-π and electrostatic interactions involving HIS32, GLN35, PHE36, LEU40, VAL150, PRO151,ALA152, LEU161 ASN162, PRO163, GLN164, GLY165, MET166, THR168, MET171, & PHE174 amino acids and hydrogen bonding between oxygen and nitrogen atoms, both compounds bonded well into the E. coli DsbA active site.

5. CONCLUSION

This study effectively synthesized three derivatives of 2-hydroxy-1, 2-diphenylethanone with considerable antibacterial activity. The highest activity of the three synthesized compounds against *Pseudomonas aeruginosa* MDR1, *Shigella soneii* 1, and *Shigella boydii* D13629 is 10µg/mL by the compound **21**. Interestingly, **22** demonstrates greater ZOI than the standard Griseofulvin against *Penicillium funiculosum* NCTC 287 strains (15.0mm) and have demonstrates similar activity against *Aspergillus niger* ATCC 6275 (15.0mm). Furthermore, the produced compounds showed advantageous interactions with the *E. coli* DsbA enzyme's active site, which is essential for bacterial protein maturation and a major participant in bacterial protein biosynthesis.

6. RECOMMENDATION

The current work recommends the following actions:

- ✓ Verify the molecular docking results experimentally.
- ✓ Produce more 2-hydroxy-1, 2-diphenylethanone and assess its possible antibacterial properties.
- ✓ Examine further possible biological activities for the three produced 2-hydroxy-1, 2-diphenylethanone molecules, such as antiviral, anticancer, anti-inflammatory, and antioxidant properties.
- ✓ Evaluate the safety profile of the produced chemicals, conduct thorough toxicity tests.

Reference

Atia Sharif, H. N., Rehman, R., Mushtaq, A., & Rashid, U. A. (2016). Review on bioactive potential of Benzoin resin. *Int. J. Chem. Biochem. Sci*, *10*, 106–110.

B., W. G. . H. (2023). *E.coli DsbA in complex with N-(2-fluorophenyl)-5-methylisoxazole-3-carboxamide*.

Babu Kothapalli, R., Anusha, B., Naveen Kumar, M., Singh, P. S., Ramakrishna, S., & Venkata Subba Reddy, U. (2025). Deracemization of Benzoin and its Derivatives via Kinetic, Dynamic Kinetic, Aerobic Oxidative Kinetic, and Reagent-mediated resolution. *Chemistry–An Asian Journal*, e202401693.

Berkelman, R. L., Bryan, R. T., Osterholm, M. T., LeDuc, J. W., & Hughes, J. M. (1994). Infectious Disease Surveillance: a Crumbling Foundation. *Science*, *264*(5157), 368–370.

Blicke, F. F. (1942). The Mannich Reaction. *Organic Reactions*, *1*, 303–341.

Buran, K. (2025). Metal complexes of sulfamethazine/benzoin-based Schiff base ligand: synthesis, characterization, DFT calculations, and antimicrobial activities. *Turkish Journal of Biology*, *49*(SI-1), 118–126.

Dong, J., Wang, N.-N., Yao, Z.-J., Zhang, L., Cheng, Y., Ouyang, D., Lu, A.-P., & Cao, D.-S. (2018). ADMETlab: a platform for systematic ADMET evaluation based on a comprehensively collected ADMET database. *Journal of Cheminformatics*, *10*, 1–11.

Fernández, C. G. (2004). Benzoin, a resin produced by Styrax trees in North Sumatra Province, Indonesia. *Forest Products, Livelihoods and Conservation: Case Studies of Non-Timber Forest Product Systems*, *1*, 148.

Garrido, A., Lepailleur, A., Mignani, S. M., Dallemagne, P., & Rochais, C. (2020). hERG toxicity assessment: Useful guidelines for drug design. *European Journal of Medicinal Chemistry*, *195*, 112290.

Jorgensen, J. H., & Turnidge, J. D. (2015). Susceptibility test methods: dilution and disk

diffusion methods. *Manual of Clinical Microbiology*, 1253–1273.

Keenan, K., Silva Corrêa, J., Sringernyuang, L., Nayiga, S., & Chandler, C. I. R. (2025). The social burden of antimicrobial resistance: what is it, how can we measure it, and why does it matter? *JAC-Antimicrobial Resistance*, *7*(2), 1–10.

Okeke, I. N., de Kraker, M. E. A., Van Boeckel, T. P., Kumar, C. K., Schmitt, H., Gales, A. C., Bertagnolio, S., Sharland, M., & Laxminarayan, R. (2024). The scope of the antimicrobial resistance challenge. *The Lancet*, *403*(10442), 2426–2438.

Paul, J. (2024). Introduction to infectious diseases. In *Disease Causing Microbes* (pp. 1–63). Springer.

Pieniążek, J. M., Padkowska, A., Dobosz, M., Arciszewska, K., Buczkowski, J., Miazga, M., Paprocki, M., & Mataczyńska, A. (2024). Overview Of The Main Bacterial Infections In Humans. *Quality in Sport*, *23*, 54786.

Rathore, A., Sharma, S., & Sharma, M. (2025). Challenges in Infectious Disease Management. In *Sustainable Nanomaterials for Treatment and Diagnosis of Infectious Diseases* pp. 51–79.

Sarsamkar, S. K., & Gramopadhye, N. S. (2021). Characterization and Antimicrobial Activity of New Cobalt-Nickel-Copper (Ii) Complexes with Benzoin and 3-Amino Benzoic Acid. *SSRN Electronic Journal*, *Ii*.

Steward, C. D., Rasheed, J. K., Hubert, S. K., Biddle, J. W., Raney, P. M., Anderson, G. J., Williams, P. P., Brittain, K. L., Oliver, A., & McGowan Jr, J. E. (2001). Characterization of clinical isolates of Klebsiella pneumoniae from 19 laboratories using the National Committee for Clinical Laboratory Standards extended-spectrum β-lactamase detection methods. *Journal of Clinical Microbiology*, *39*(8), 2864–2872.

Trott, O., & Olson, A. J. (2010). AutoDock Vina: Improving the speed and accuracy of docking with a new scoring function, efficient optimization, and multithreading. *Journal of Computational Chemistry*, *31*(2), 455–461.

WHO. (2024). WHO bacterial priority pathogens list, 2024. In *Bacterial pathogens of public health importance to guide research, development and strategies to prevent and control antimicrobial resistance*.

Wiegand, I., Hilpert, K., & Hancock, R. E. W. (2008). Agar and broth dilution methods to determine the minimal inhibitory concentration (MIC) of antimicrobial substances. *Nature Protocols*, *3*(2), 163–175.

Yaylı, N., Kahriman, N., Kılıç, G., Serdaroğlu, V., Aliyazıcıoğlu, R., Sellitepe, H. E., Karaoğlu, Ş. A., & Yılmaz, G. T. (2022). Molecular docking, synthesis and biological evaluation (enzyme inhibition, antimicrobial and antioxidant) of methoxy benzoin/benzil/stilbenoid derivatives. *Organic Communications*, *15*(2), 129–147.

Zaware, N., Rasal, N., Lambate, V., & Jagtap, S. (2025). Biological evaluation of newly synthesized α-benzil monoxime thiocarbohydrazide derivatives as an antimicrobial and anticancer agent: In vitro screening and ADMET predictions. *Bioorganic & Medicinal Chemistry Letters*, *118*, 130079.